



HAL
open science

Intracerebral electrical stimulation of the right anterior fusiform gyrus impairs human face identity recognition

Angélique Volfart, Xiaoqian Yan, Louis Maillard, Sophie Colnat-Coulbois,
Gabriela Hossu, Bruno Rossion, Jacques Jonas

► **To cite this version:**

Angélique Volfart, Xiaoqian Yan, Louis Maillard, Sophie Colnat-Coulbois, Gabriela Hossu, et al.. Intracerebral electrical stimulation of the right anterior fusiform gyrus impairs human face identity recognition. *NeuroImage*, 2022, 250, pp.118932. 10.1016/j.neuroimage.2022.118932 . hal-03863185

HAL Id: hal-03863185

<https://hal.science/hal-03863185>

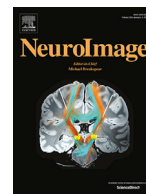
Submitted on 21 Nov 2022

HAL is a multi-disciplinary open access archive for the deposit and dissemination of scientific research documents, whether they are published or not. The documents may come from teaching and research institutions in France or abroad, or from public or private research centers.

L'archive ouverte pluridisciplinaire **HAL**, est destinée au dépôt et à la diffusion de documents scientifiques de niveau recherche, publiés ou non, émanant des établissements d'enseignement et de recherche français ou étrangers, des laboratoires publics ou privés.



Distributed under a Creative Commons Attribution 4.0 International License



Intracerebral electrical stimulation of the right anterior fusiform gyrus impairs human face identity recognition

Angélique Volfart^{a,b}, Xiaoqian Yan^{a,b,c}, Louis Maillard^{a,d}, Sophie Colnat-Coulbois^{a,e}, Gabriela Hossu^{f,g}, Bruno Rossion^{a,b,d,1}, Jacques Jonas^{a,d,1,*}

^a Université de Lorraine, CNRS, CRAN, F-54000 Nancy, France

^b University of Louvain, Psychological Sciences Research Institute, Louvain-La-Neuve B-1348, Belgium

^c Department of Psychology, Stanford University, Stanford, CA 94305, USA

^d Université de Lorraine, CHRU-Nancy, Service de Neurologie, F-54000 Nancy, France

^e Université de Lorraine, CHRU-Nancy, Service de Neurochirurgie, F-54000 Nancy, France

^f Université de Lorraine, CHRU-Nancy, CIC-IT, Nancy F-54000, France

^g Inserm, IADI, Université de Lorraine, Nancy F-54000, France

ARTICLE INFO

Keywords:

Anterior fusiform gyrus
Electrical brain stimulation
Face identity recognition
SEEG

ABSTRACT

Brain regions located between the right fusiform face area (FFA) in the middle fusiform gyrus and the temporal pole may play a critical role in human face identity recognition but their investigation is limited by a large signal drop-out in functional magnetic resonance imaging (fMRI). Here we report an original case who is suddenly unable to recognize the identity of faces when electrically stimulated on a focal location inside this intermediate region of the right anterior fusiform gyrus. The reliable transient identity recognition deficit occurs without any change of percept, even during nonverbal face tasks (i.e., pointing out the famous face picture among three options; matching pictures of unfamiliar or familiar faces for their identities), and without difficulty at recognizing visual objects or famous written names. The effective contact is associated with the largest frequency-tagged electrophysiological signals of face-selectivity and of familiar and unfamiliar face identity recognition. This extensive multimodal investigation points to the right anterior fusiform gyrus as a critical hub of the human cortical face network, between posterior ventral occipito-temporal face-selective regions directly connected to low-level visual cortex, the medial temporal lobe involved in generic memory encoding, and ventral anterior temporal lobe regions holding semantic associations to people's identity.

1. Introduction

In our human species, recognizing people's identity by their faces is key for social interactions. This face identity recognition (FIR) function is extremely challenging because of the visual similarity among the many individual faces encountered, their complex configuration with multiple features varying in shape, texture and color cues, and the large changes of viewing appearances of a given person's face. Despite this challenge, neurotypical human adults attain a high degree of proficiency at recognizing familiar face identities: they can recognize thousands of identities from their faces (Jenkins et al., 2018), within a

fraction of a second and automatically (e.g. Barragan-Jason et al., 2013; Caharel et al., 2014; Zimmermann et al., 2019). The neural basis of this impressive recognition function has been initially investigated by studies of patients with a specific FIR impairment following brain damage, i.e., prosopagnosia (Bodamer, 1947). Collectively, these lesion studies point to a crucial role of the ventral occipito-temporal cortex (VOTC), in particular the hominoid-specific fusiform gyrus (FG), with a dominant contribution of the right hemisphere (Meadows, 1974; Sergent and Signoret, 1992; Bouvier and Engel, 2006; Barton, 2008; Cohen et al., 2019; see Rossion, 2014 for review).

In agreement with these observations, neuroimaging studies, mainly with functional magnetic resonance imaging (fMRI), have consistently

AntCOS, Anterior section of the Collateral Sulcus; AntFG, Anterior section of the Fusiform Gyrus; AntOTS, Anterior section of the Occipito-Temporal Sulcus; ATL, Anterior Temporal Lobe; FFA, Fusiform Face Area; FFT, Fast Fourier Transform; FG, Fusiform Gyrus; FIR, Face Identity Recognition; fMRI, functional Magnetic Resonance Imaging; FPVS, Fast Periodic Visual Stimulation; OFA, Occipital Face Area; SEEG, Stereotaxic Electroencephalography; tSNR, temporal Signal-to-Noise Ratio; VOTC, Ventral Occipito-Temporal Cortex.

* Corresponding author at: Université de Lorraine, CNRS, CRAN, CHRU-Nancy, Hôpital Central, 29 avenue du Maréchal de Lattre de Tassigny, F-54000 Nancy, France

E-mail address: jacques.jonas@univ-lorraine.fr (J. Jonas).

¹ These authors contributed equally to this work.

<https://doi.org/10.1016/j.neuroimage.2022.118932>

Received 16 June 2021; Received in revised form 17 January 2022; Accepted 23 January 2022

Available online 24 January 2022.

1053-8119/© 2022 Published by Elsevier Inc. This is an open access article under the CC BY-NC-ND license (<http://creativecommons.org/licenses/by-nc-nd/4.0/>)

reported face-selective activity (i.e., larger neural responses to faces than non-face stimuli) in the posterior VOTC. Specifically, these face-selective clusters have been systematically found in the inferior occipital gyrus (“occipital face area” or OFA, Gauthier et al., 2000) and in the lateral section of the posterior and middle FG (“fusiform face area” or FFA, Kanwisher et al., 1997; or “pFus-faces” and “mFus-faces”, Weiner and Grill-Spector, 2012a; for review: Grill-Spector et al., 2017). In the last decade, face-selective clusters in more anterior regions of the VOTC, i.e., in the ventral anterior temporal lobe (ventral ATL), have also been reported, usually close to the temporal pole (Rajimehr et al., 2009; Nasr and Tootell, 2012; Rossion et al., 2012; Avidan et al., 2014), supporting suggestive evidence from lesion studies that ventral ATL regions may also be important for FIR (Barton, 2008; Busigny et al., 2014; Cohen et al., 2019). However, given their very anterior localization (i.e., close to the temporal pole) and their multimodal response properties, these ventral ATL regions have been linked to multimodal person-recognition (person semantic knowledge) rather than to visual FIR *per se* (Collins and Olson, 2014; Collins et al., 2016; Rice et al., 2018; see also Gainotti et al., 2010; Gainotti, 2013a).

Critically, an overview of fMRI-based face-selective activity in the human brain points to a substantial spatial “gap” between the FFA/mFus-faces and the ventral ATL face-selective area(s) close to the temporal pole. This gap in functional activity corresponds in particular to the location of the anterior section of the FG (AntFG; Fig. 1A). While this region may correspond to a transition zone between perceptual and memory-based aspects of FIR (and of hypothetical apperceptive and associative forms of prosopagnosia, respectively; Davies-Thompson et al., 2014), it also corresponds, unfortunately, to a location affected by a large signal drop-out arising from magnetic susceptibility artifacts in fMRI (Fig. 1B; Wandell, 2011; Axelrod and Yovel, 2013; Rossion et al., 2018). Consequently, even with distortion-corrected fMRI sequences improving signal-to-noise ratio in the ventral ATL (e.g., Embleton et al., 2010; Hoffman and Lambon Ralph, 2018), face-selectivity remains low or invisible specifically in this AntFG region (Collins et al., 2016; Rice et al., 2018; see discussion in Rossion et al., 2018) limiting its deeper exploration and understanding with this technique (Fig. 1C–E; for recent illustrations of this functional spatial gap in face-selectivity, see also Figs. 1 and 4 in Wang et al., 2020).

Beyond fMRI, a few sources of evidence nevertheless point to a functional role of the AntFG, in particular in the right hemisphere, in human FIR. First, two early studies using positron emission tomography identified the AntFG in a contrast between familiar and unfamiliar faces (Wiser et al., 2000; Rossion et al., 2001). In the latter study, the right AntFG signaled a clear-cut (i.e., categorical) difference between familiar and unfamiliar faces in an orthogonal task (Rossion et al., 2001), in a region that was clearly demarcated (i.e., located anteriorly) from the FFA/mFus-faces cluster (Rossion et al., 2003). Second, a volume reduction of the AntFG has been specifically reported in FIR impairments of neurodevelopmental origin (i.e., prosopagnosia), correlating with behavioral decrement in this function (Behrmann et al., 2007). Third, more recently, intracerebral electrical stimulation of a face-selective electrode implanted in the right AntFG of a single case induced a spectacular transient FIR inability (Jonas et al., 2015). Importantly, unlike other reports about the effect of electrical stimulations on posterior face-selective VOTC regions, the subject did not report any change in perceptual experience of faces (e.g., rearrangement of facial feature as in Jonas et al., 2012; distortions as in Parvizi et al., 2012; Rangarajan et al., 2014; Schalk et al., 2017; Schrouff et al., 2020; face identity palinopsia as in Jonas et al., 2018; see Jonas and Rossion, 2021 for review). Finally and most recently, frequency-tagging intracerebral electroencephalography (EEG) studies using depth electrodes (stereotaxic EEG or SEEG, Talairach and Bancaud, 1973) with large groups of patients have disclosed relatively large face-selective activity in the right AntFG (Jonas et al., 2016; Hagen et al., 2020), as well as a high sensitivity to differences between unfamiliar face identities (Jacques et al., 2020).

Collectively, while these observations suggest a significant contribution of the right AntFG in human FIR, the critical and specific role of this region in this function remains largely unknown. To shed light on this issue, here we provide an extensive multimodal investigation (behavior, SEEG recordings and stimulation, fMRI) in a case of transient FIR impairment during focal electrical stimulation of the right AntFG. While the electrode contacts leading to the transient FIR failure are located in the same region as the only previously reported case (Jonas et al., 2015), the present case report goes well beyond this initial report. Specifically, here we provide a systematic and extensive behavioral investigation during stimulation with multiple tasks (quantified in terms of both accuracy rates and response times), fMRI recordings, as well as an objective quantification of frequency-tagged face-selective, unfamiliar face discrimination and famous face identity electrophysiological responses on the effective contacts. Altogether, these investigations provide substantial unique evidence and clarification for the critical role of the right AntFG in human FIR.

2. Materials and methods

2.1. Case description

The subject was a right-handed 40-year-old man (DN) with refractory focal epilepsy. As part of the clinical investigation of his epilepsy, DN underwent a SEEG in August 2018. Following SEEG exploration, the epileptogenic zone was delineated in the left ATL. DN gave written consent for the experimental procedures that were administered during his SEEG exploration and were part of the clinical investigation as approved by the ethical committee of the University Hospital of Nancy. He also gave written consent for the fMRI experiment and the use of video material.

2.2. Neuropsychological assessment

2.2.1. General assessment

DN showed a general intellectual efficiency in the low-normal range (total IQ of 83; WAIS-IV), with a verbal/nonverbal IQ discrepancy (verbal IQ: 104 > non-verbal IQ: 82). Neuropsychological assessment showed normal performance in verbal and nonverbal memory (Grober & Buschke Free and Cued Selective Reminding Test, Brief Visuospatial Memory Test-Revised). He was slightly slowed down at processing visuo-spatial information (subtest Code, WAIS-IV, percentile 5). He performed below the normal range at naming objects (74/80 at the DO80 naming test, $z = -2.69$), consistent with the left lateralization of his epileptogenic zone in the temporal lobe. Importantly, he never complained of FIR difficulties, neither in his daily life nor during/after epileptic seizures.

2.2.2. Face recognition

Outside the SEEG procedure, a series of behavioral tests were performed to specifically assess DN's performance at face/object recognition. These tests included (1) the electronic version of the Benton Facial Recognition Test (BFRT-c; Rossion and Michel, 2018); (2) a delayed matching task with pictures of faces and cars at upright and inverted orientations (Experiment 4 in Busigny and Rossion, 2010); (3) a simultaneous matching task with famous and unfamiliar faces at upright and inverted orientations; (4) a face memory task; (5) a famous face pointing task; and (6) a famous name pointing task (see all methods in **Supplementary Information**). All tasks were administered through E-Prime 2.0 on a 60 Hz screen, at a distance of about 60 cm.

We also tested five control participants (matched on gender, age, handedness and educational level) with the same tests. To compare the results of DN to the control participants, a modified *t*-test of Crawford and Howell for single-case studies was used (Crawford and Howell, 1998; Crawford and Garthwaite, 2002), with a *p* value below 0.05 (one-tailed) considered as statistically significant.

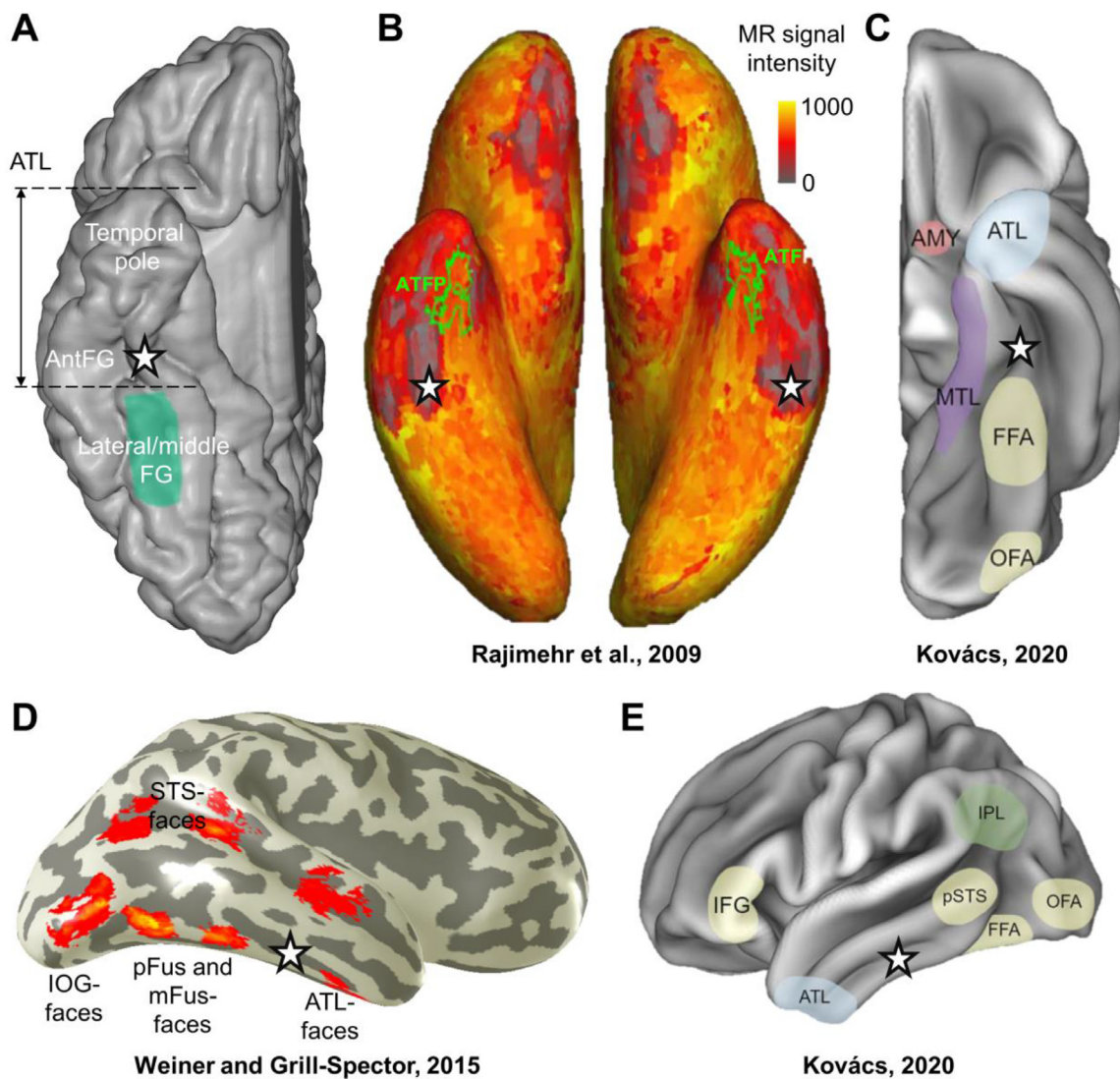


Fig. 1. Anatomical location of the AntFG and its spatial relationship with classical fMRI face-selective regions and fMRI signal drop-out. **A.** The anatomical location of the AntFG (black and white star) is shown on a transparent reconstructed cortical surface of the Colin27 brain (ventral view). The AntFG is located in the posterior section of the ATL, just anteriorly to the lateral section of the middle FG, i.e., the typical location of the FFA. **B.** The approximate location of the AntFG is indicated on an inflated view of the VOTC (Rajimehr et al., 2009). The AntFG is located posteriorly to the classical ATL face-selective activations identified with fMRI, usually located very anteriorly, close to the temporal pole (ATFP, green outlines), and within a strong magnetic susceptibility artifact due to the ear canal, i.e., signal drop-out, affecting the ventral ATL (grey zones). Consequently, fMRI studies rarely report the AntFG as face-selective and usually report a gap between the FFA (pFus and mFus-faces) and the classical ATL face-selective activations. **C.** The approximate location of the AntFG is indicated on a recent illustration of the cortical face network based on fMRI studies, ventral view (Kovács, 2020). **D.** The approximate location of the AntFG is indicated on an inflated lateral brain view, along with the classical face-selective activations found in fMRI (Weiner and Grill-Spector, 2015). **E.** Same as panel C, lateral view (Kovács, 2020).

DN performed extremely well at all tasks with upright faces both in accuracy and response times, and was in the normal range for all of these tasks (even regularly outperforming controls, **Supplementary Table 1**). Overall, these results indicate that DN has normal FIR ability.

2.3. Stereotaxic placement of intracerebral electrodes

Intracerebral depth electrodes were stereotaxically implanted in DN's brain in order to delineate the seizure onset zone (Talairach and Bancaud, 1973; Cardinale et al., 2012; Salado et al., 2017). The sites of electrode implantation were determined based on non-invasive data collected during an earlier phase of the investigation. Each intracerebral electrode consisted of a cylinder of 0.8 mm diameter and contained a linear array of 8–15 recording contacts, each 2 mm in length separated by 1.5 mm from edge to edge (Dixi Medical, Besançon, France). The implantation was performed exactly as in previous procedures (e.g.,

Salado et al., 2017). A postoperative non-stereotaxic CT-scan was carried out and fused with a T1-weighted MRI to determine the exact anatomical position of each electrode.

Twelve electrodes were implanted in total in DN's brain, including six electrodes in the left VOTC and three electrodes in the right VOTC (TM, TB, and B). Electrode TM (15 contacts) was located in the right ventral ATL and targeted specifically the anterior collateral sulcus (AntCOS), the AntFG, the anterior occipito-temporal sulcus (AntOTS) and the inferior temporal gyrus (see Fig. 2A). Electrode TB (11 contacts) also explored the ventral ATL and was located anteriorly to electrode TM. Electrode B (15 contacts) targeted the body of the right hippocampus.

The SEEG signal was recorded at a 512 kHz sampling rate on a 256-channel amplifier (4 SD LTM 64 Headbox, Micromed, Treviso, Italy). The reference electrode during data acquisition was an intracerebral contact located in the white matter of the right ATL.

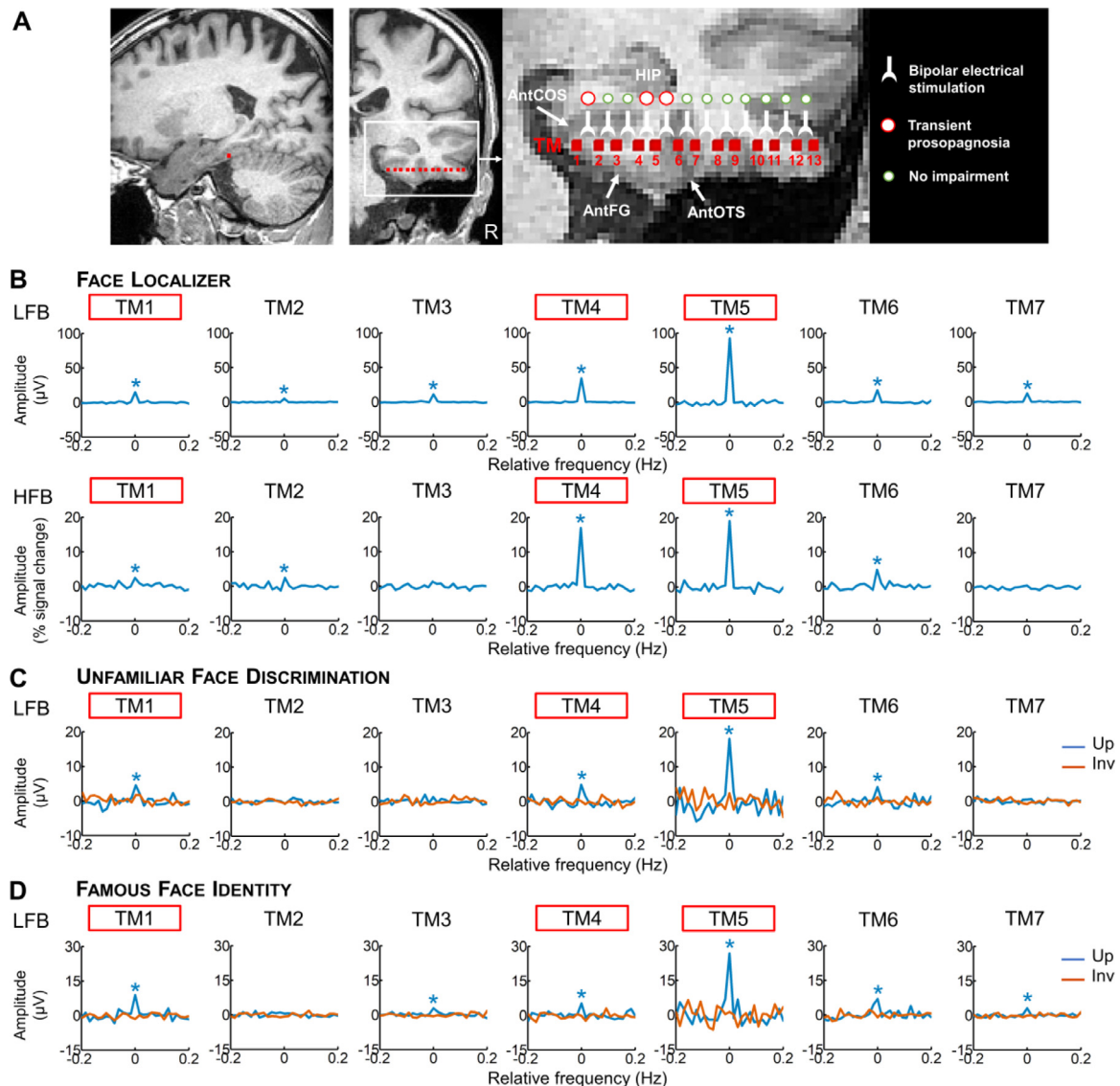


Fig. 2. Anatomical and functional location of the stimulation sites inducing transient prosopagnosia. **A.** Anatomical location of electrode TM (in red) in sagittal and coronal MRI slices. AntCOS, anterior part of the collateral sulcus; AntFG, anterior part of the fusiform gyrus; AntOTS, anterior part of the occipito-temporal sulcus; HIP, hippocampus. **B.** Face-selective intracerebral responses (Face Localizer experiment, see Fig. 4A) recorded on electrode TM in low-frequency bands (LFB, above) and in high-frequency bands (HFB, below). These responses were determined by summing segments of the EEG spectrum centered on the face presentation frequency and its harmonics (i.e., 1.2, 2.4, 3.6, and 4.8 Hz). The 0 mark corresponds to the face presentation frequency. Note the particularly large face-selective response in both low- and high-frequency bands for the contacts whose stimulation induces transient prosopagnosia, and especially for the effective contact TM5. **C.** Intracerebral LFB responses to unfamiliar face discrimination (Unfamiliar Face Discrimination experiment, see Fig. 4B) recorded on electrode TM for both upright and inverted faces. The contacts inducing transient prosopagnosia, in particular TM5, were sensitive to unfamiliar face discrimination for upright faces only. **D.** Intracerebral LFB responses to famous face identity recognition (Famous Face Identity experiment, see Fig. 4C) recorded on electrode TM for both upright and inverted faces. Contacts inducing transient prosopagnosia were sensitive to famous faces for upright faces only, in particular TM5. Red rectangles around contact's name represent contacts on which electrical stimulation elicited transient FIR impairment. (*) indicates significant responses at $p < .001$.

2.4. Intracerebral electrical stimulations

2.4.1. General procedure

Intracerebral electrical stimulations were applied at 1.2 mA between two adjacent contacts as biphasic square wave pulses with 1050 μ s width (alternating positive and negative 500 μ s phases, spaced from each other by 25 μ s) delivered at 55 Hz during 5 s (except for 3 out of 42 stimulations that lasted 10 s). These stimulation parameters are typical in SEEG (Trébuchon and Chauvel, 2016; Isnard et al., 2018; Ritaccio et al., 2018; So and Alwaki, 2018; Grande et al., 2020; Aron et al., 2021) and were also used in our previous reports eliciting transient FIR impairments (Jonas et al., 2012, 2015, 2018). While presented with a set of succes-

sive images, DN was not aware of the exact stimulation onset, duration and termination (no pain during stimulation, no click sound at onset, etc.). He was never made aware of the stimulation site or the nature of the impairments that could potentially be elicited during electrical stimulations.

Before, during and after each intracerebral electrical stimulation of electrode TM contacts, DN was asked to perform several trials of a pre-specified task involving successive images of faces, objects, buildings and written names (i.e., pointing out famous faces and names, Fig. 3A; matching unfamiliar or famous faces, Fig. 3B; naming famous faces, famous buildings and visual objects). Considering the limited amount of time afforded by the clinical context, we first identified the relevant elec-

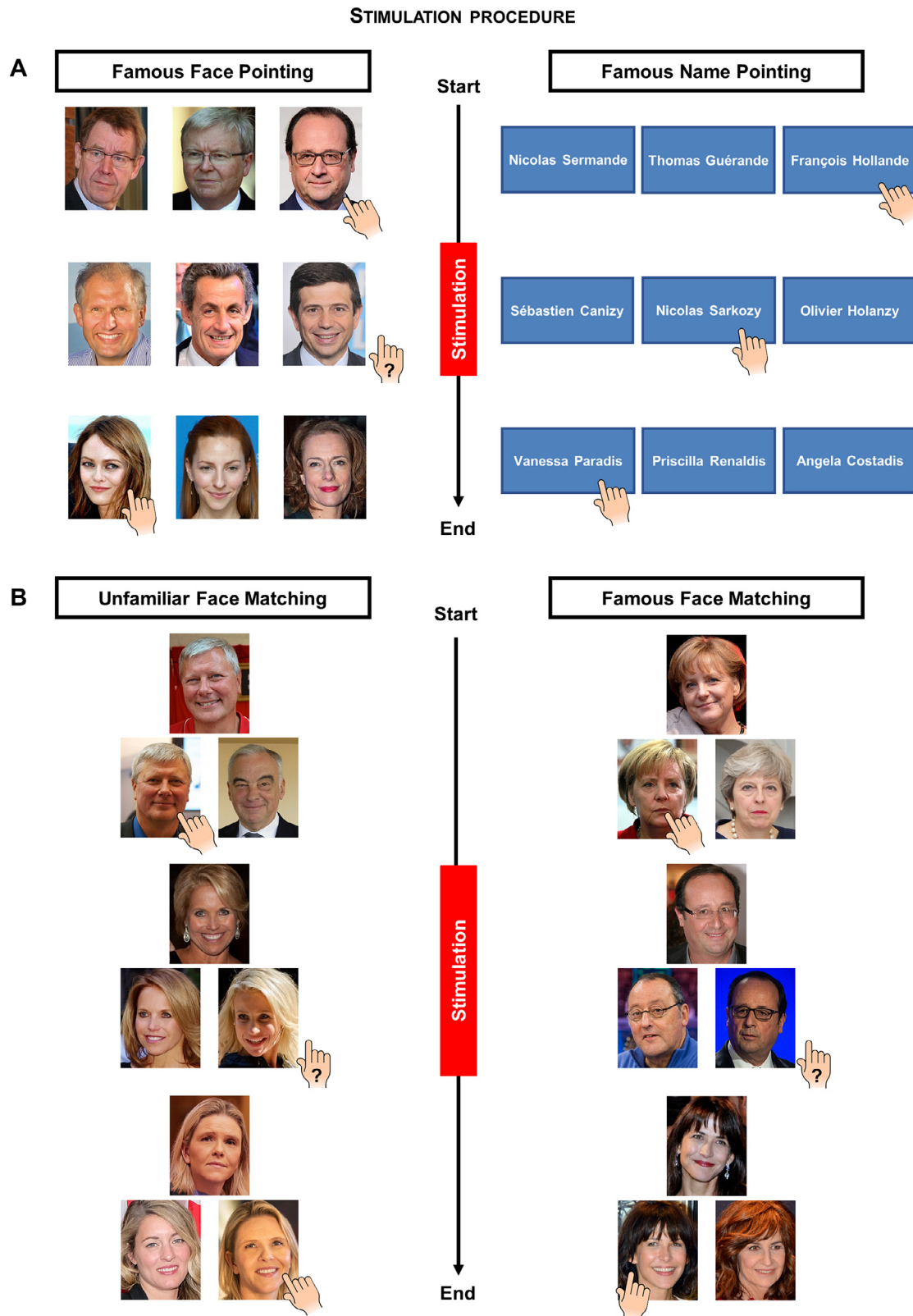


Fig. 3. Stimuli and procedure of the famous pointing tasks (face and name) and simultaneous face matching tasks (famous and unfamiliar) performed during stimulation sessions on electrode TM contacts. A. Famous face and name pointing tasks. DN had to point to the famous item presented among two unfamiliar distractors, before, during and after electrical stimulation of two adjacent intracerebral contacts. B. Unfamiliar and famous face matching tasks. Each trial consisted of three face photographs organized in two rows with a target on the top and two probes on the bottom, with one of the probes being another photograph of the target identity and the other probe being a photograph of another identity. DN had to match the probe with the target by pointing to the correct face, before, during and after electrical stimulation of two adjacent intracerebral contacts. Note that the pictures used in this figure were not those used in the original paradigm because of copyright reasons (copyright information for the pictures shown here are available in Supplementary Information).

trode contacts for FIR with one task (pointing to the famous face) and then further tested these contacts with the remaining tasks. Given that DN was flawless outside of stimulation, and in line with his high performance at neuropsychological tests of face recognition (**Supplementary Table 1**), we considered that a stimulation evoked an impairment if he failed (error or no response) at least one trial during the time of the stimulation. Since we found a FIR impairment with the pointing task when stimulating the first electrode tested, i.e., electrode TM (**Fig. 2A**), we focused on this electrode to maximize the number of relevant tasks and trials (i.e., other electrodes were not stimulated with face-related tasks).

The stimulation sites, the number of stimulations performed at each stimulation site and type of task used are presented in **Supplementary Table 2**. Below, we describe the different face and non-face tasks performed during stimulation sessions. The neurologist (JJ) performed all electrical stimulations and set the stimulation site, the stimulation parameters, the task, and the onset of the stimulation. For each stimulation and task, we measured the accuracy and the response times before, during and after stimulation by retrospectively rewatching the video recording (for response times, we measured the delay between the presentation of the trial and either when the finger touched the image or when the subject finished naming, depending on the task).

2.4.2. Famous face and famous name pointing tasks

The same tasks as used to evaluate FIR performance outside the SEEG procedure (100% of accuracy, see Neuropsychological assessment section, **Supplementary Information and Supplementary Table 1**) were used during stimulation sessions. Each trial consisted of 3 faces or written names presented next to each other, with one famous and 2 unfamiliar identities (**Fig. 3A**). The famous identity on each trial was the same across modalities (faces and names). Face images were 5.7 cm wide by 7.7 cm high; written names ranged from 2.1 to 5.6 cm in width, and from 0.4 to 1.3 cm in height. For each stimulation session, DN was presented with a set of 3 to 10 trials of the same category (faces or names), presented one by one, and he had to point to the famous face or name in turn (**Fig. 3A**). For each set, the electrical stimulation was randomly triggered during the presentation of 1 to 3 trials.

In total, DN was presented with 153 face trials (across 24 stimulation sessions on electrode TM contacts): 44 during electrical stimulation, 41 before and 68 after (since there were 50 different face trials in total, several face trials were repeated across stimulation sessions). DN was also presented with 52 name trials (across 7 stimulation sessions): 17 during electrical stimulation, 18 before and 17 after.

Immediately after stimulating one site (TM4-TM5), DN was presented again with several trials presented during the stimulation session along with distractors and he was asked to indicate verbally if these trials had been presented during the stimulation session or not. This recall task was performed after 8 stimulation sessions with faces, and 7 with names. He was also presented again with the missed trials (no response or error) and asked to perform the task again. This was done after 5 TM4-TM5 stimulation sessions with faces.

2.4.3. Famous and unfamiliar face matching tasks

These tasks were the same as those used during the FIR evaluation outside the SEEG procedure (100% of accuracy, see Neuropsychological assessment section, **Supplementary Information and Supplementary Table 1**), except that only upright faces were presented.

Each trial consisted of three face photographs organized with a target on top of two probes: another face photograph of the target identity vs. a face distractor (**Fig. 3B**). Face images were 7 cm wide by 9 cm high. For each stimulation session, DN was presented with a set of 6 to 9 trials of the same category (famous or unfamiliar), presented one by one, and he had to point to the probe corresponding to the target (**Fig. 3B**). For each set, the electrical stimulation was randomly triggered during the presentation of 2 to 5 trials. Note that the two stimulations triggered during unfamiliar face matching lasted 10 s instead of 5 s.

In total (across 4 stimulation sessions of electrode TM contacts), DN was presented with 15 unfamiliar face trials (across 2 stimulation sessions of contacts TM4-5) and 16 famous face trials (2 stimulation sessions of contacts TM4-5), corresponding to 8 unfamiliar and 4 famous trials during stimulation, 4 and 7 before, and 3 and 5 after. Twenty-two images were available for each set so that no face trials were repeated across stimulation sessions.

Immediately after each stimulation session, DN was presented again with several trials presented during the stimulation procedure along with distractors. He was asked to indicate verbally if these trials had been presented during the stimulation session or not. He was also presented again with two famous face trials on which he hesitated (1 stimulation session), and asked to perform the task again.

2.4.4. Famous face, famous building and object naming

Stimulations were also carried out during recognition of sets of images of the same category presented one by one (famous faces, famous buildings, or visual objects; see **Supplementary Fig. S1 for examples**). DN had to name each image in turn. Face images were 13.4 cm wide by 15 cm high; visual objects ranged from 2.5 to 13.5 cm in width, and from 1 to 7.5 cm in height; famous building images measured between 9.3 and 15.7 cm wide, and between 9.8 and 12.5 cm high. For each set, the stimulation was randomly triggered during the presentation of 2 to 4 images.

In total (across 7 stimulation sessions on electrode TM contacts), DN was presented with 25 pictures of isolated famous faces (3 stimulation sessions: 6 images during electrical stimulation, 9 before and 10 after; one image was presented twice across 2 stimulation sessions), 27 visual objects (including animals and fruits/vegetables; 3 stimulation sessions: 9 images during, 8 before and 10 after; 4 images were presented twice across 2 stimulation sessions) and 8 famous buildings (1 stimulation session: 2 images during, 3 before and 3 after; no repetition of images).

Immediately after 6 out of 7 stimulation sessions, DN was again presented with several images presented during the stimulation session along with distractors and was asked to indicate verbally if these trials had been presented during the stimulation session or not.

2.5. Fast periodic visual stimulation: intracerebral responses

2.5.1. FPVS paradigms: stimuli and procedure

Well-validated fast periodic visual stimulation (FPVS) (or “frequency-tagging”; see **Norcia et al., 2015; Rossion et al., 2020**) paradigms were used to identify face-selective contacts and contacts sensitive to unfamiliar face discrimination and famous face identity recognition (**Fig. 4**, see also **Supplementary Information** for all methods details). These recordings were performed on the day before the electrical stimulation sessions (but note that electrical stimulation sessions were performed blind to the results of the FPVS paradigms).

Face-selective responses were recorded with 70 s sequences of variable non-face object images presented at 6 Hz while inserting periodically (every 5 images) widely variable natural images of face stimuli, so that the face frequency among objects was set at 1.2 Hz, i.e., 6 Hz / 5 (Face Localizer experiment, **Fig. 4A**). This paradigm was run exactly as in previously described intracerebral recording group studies (**Jonas et al., 2016; Hagen et al., 2020**). Unfamiliar face discrimination neural responses were recorded with a paradigm presenting the same unfamiliar face identity at a fast 6 Hz rate while periodically inserting (every 5 images) different unfamiliar face identities, so that the frequency of identity change was set at 1.2 Hz, i.e., 6 Hz / 5 (Unfamiliar Face Discrimination experiment; **Liu-Shuang et al., 2014; Rossion et al., 2020; Fig. 4B**). Faces were presented either at upright or inverted orientation in separate sequences. This paradigm was run exactly as in a previously described intracerebral recording group study (**Jacques et al., 2020**). Finally, responses reflecting sensitivity to famous face identity were recorded by presenting variable images of unfamiliar faces also at 6 Hz, with different exemplars of the same famous identity appearing

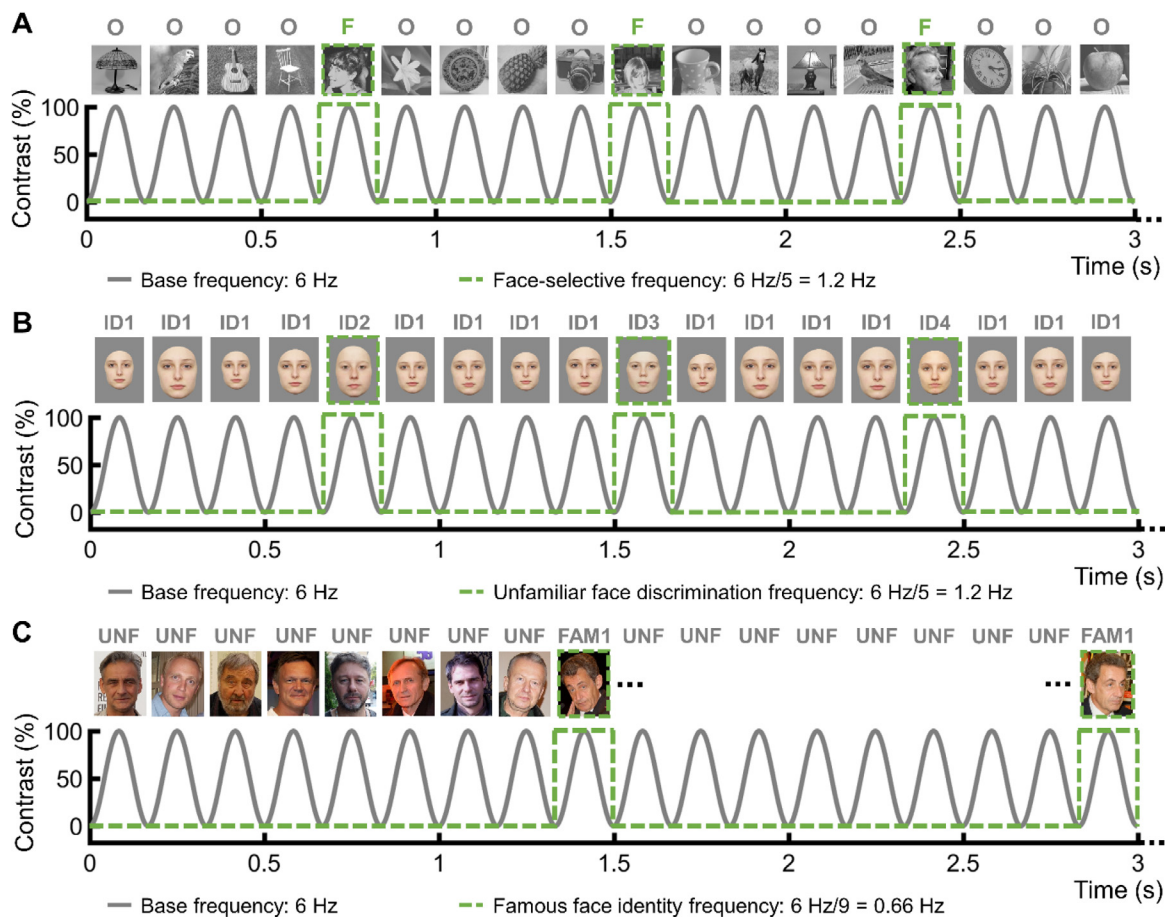


Fig. 4. FPVS paradigms during SEEG recordings. **A.** Face Localizer paradigm used to define face-selective neural activity (Rossion et al., 2015). **B.** Unfamiliar Face Discrimination paradigm used to measure sensitivity to unfamiliar face identity changes (Liu-Shuang et al., 2014; Rossion et al., 2020). Faces were presented either in upright or inverted orientation in separate sequences (only the upright condition is shown here). **C.** Famous Face Identity paradigm used to measure sensitivity to individual famous faces (Zimmermann et al., 2019). Faces were presented either in upright or inverted orientations in separate sequences (only the upright condition is shown here). Note that the pictures used in this figure were not those used in the original paradigm because of copyright reasons. For license information, Nicolas Sarkozy: Pictures licensed under the CC BY 2.0. Attribution: Thomas Bresson. Robert Goner, Piotr Adamczyk, Krzysztof Kowalewski, Cezary Pazura, Andrzej Piacezny, and Andrzej Chyra: Pictures licensed under the CC BY-SA 2.0. Attribution: Fryta 73. Pawel Delag, and Linda Boguslaw: Pictures licensed under the CC BY-SA 2.0. Attribution: Slawek.

every 9 stimuli, so that the famous face frequency among unfamiliar faces was set at 0.666 Hz, i.e., 6 Hz / 9 (Famous Face Identity experiment; Zimmermann et al., 2019; Fig. 4C). Faces were also presented either at upright or inverted orientation in separate sequences. During all these FPVS paradigms, DN was fixating a small black cross presented continuously at the center of the stimuli and had to detect brief color-changes of this fixation cross, so that neural responses were measured without explicit task.

2.5.2. Analysis in the low-frequency bands

Preprocessing: Analyses were carried out using the free software *Letswave 5*, with a similar procedure as in recent reports (e.g., Lochy et al., 2018; Hagen et al., 2020; Jacques et al., 2020). Portions of SEEG corresponding to sequences of FPVS presentation (70 s duration) were first extracted using segments exceeding the actual visual presentation length (78 s segments, -2 s to +76 s) and then cropped to an integer number of cycles beginning after the 2 s fade-in and ending before the 2 s fade-out (i.e., ending up with 66 s segments; Face Localizer and Unfamiliar Face Discrimination = 33,707 bins; Famous Face Identity = 33,792). These sequences, acquired with a monopolar montage (reference electrode: intracerebral contact within the white matter) were re-referenced to a bipolar montage (minus the signal recorded at the contact located just laterally along the electrode). Sequences corresponding to the same condition were averaged in the time domain. A

Fast Fourier Transform (FFT) was then applied to these averaged segments and amplitude spectra were extracted for all contacts.

Identification of significant responses in the low-frequency bands: Face-selective, unfamiliar face discrimination or famous face identity responses significantly above noise level at the target frequency and its harmonics were determined in each condition as follows: (1) the FFT spectrum was cut into segments of 50 bins centered at the response frequencies (i.e., 1.2 Hz for the Face Localizer and Unfamiliar Face Discrimination paradigms, 0.666 Hz for Famous Face Identity) and harmonics, until the last harmonic before 6 Hz base frequency: 4 harmonics for the Face Localizer and Unfamiliar Face Discrimination paradigms, 8 harmonics for Famous Face Identity; (2) the amplitude values of these FFT segments were summed; (3) the summed FFT spectrum was transformed into a Z-score. Z-scores were computed as the difference between the amplitude at the target frequency bin and the mean amplitude of the 48 surrounding bins (25 bins on each side, i.e., 50 bins, excluding the first bin directly adjacent to the bin of interest, i.e. 48 bins) divided by the standard deviation of amplitudes in the corresponding 48 surrounding bins (see also Lochy et al., 2018). A contact was considered as showing a significant response in a given condition if the Z-score at the target frequency bin exceeded 3.1 ($p < 0.001$).

Quantification of response amplitudes: The responses were quantified at each contact on the sum of harmonics (Retter and Rossion, 2016; Retter et al., 2021). The range over which frequency harmonics were

summed extended from the first harmonic to the last harmonic before the base frequency (4 harmonics for the Face Localizer and Unfamiliar Face Discrimination paradigms, 8 harmonics for the Famous Face Identity paradigm). A baseline correction was then computed as the difference between the amplitude at each frequency bin and the average of the 48 surrounding bins (25 bins on each side, i.e., 50 bins, but excluding the 2 bins directly adjacent to the bin of interest, i.e., 48 bins).

Statistical comparison between upright and inverted response amplitudes: For the Unfamiliar Face Discrimination and Famous Face Identity paradigms, we statistically compared the amplitudes of the target responses at the upright and inverted conditions on each contact. To do so, the upright and inverted summed FFT segments were subtracted from one another (upright – inverted) and transformed into a Z-score. A contact was considered as showing a larger amplitude at the upright than at the inverted condition if the Z-score at the target frequency bin exceeded 3.1 (i.e., $p < 0.001$, one-tailed: upright > inverted).

2.5.3. Analysis of high-frequency broadband (“Gamma”) activity

Since low- and high-frequency face-selective responses may not always spatially overlap and may potentially reflect different functional processes in the cortical face network (Engell and McCarthy, 2011), we also examined face-selective responses in high-frequency broadband activity (“gamma range”; 30–160 Hz). To do so, we tested for periodic burst of gamma activity during the Face Localizer, Unfamiliar Face Discrimination and Famous Face Identity paradigms.

Event-related spectral perturbations were computed with *Letswave* 5. Variation in signal amplitude as a function of time and frequency was estimated by a Morlet wavelet transform on each SEEG segment, re-referenced to a bipolar montage, from frequencies of 1 to 160 Hz, in 2 Hz increments. The number of cycles (i.e., central frequency) of the wavelet was adapted as a function of frequency from 2 cycles at the lowest frequency to 9 cycles at the highest frequency. The wavelet transform was computed on each time-sample and the resulting amplitude envelope was downsampled by a factor of 12 (i.e., to a 42.6 Hz sampling rate). Amplitude was normalized across time and frequency to obtain the percentage of power change generated by the stimulus onset relative to the mean power in a pre-stimulus time-window (-1600 ms to -300 ms relative to the onset of the stimulation sequence). Then, the amplitude was averaged across frequencies (between 30 Hz and 160 Hz), the high-frequency band envelopes corresponding to the same condition were averaged in the time domain, and the frequency content of the high-frequency band envelopes was transformed using a Fast Fourier transform.

Periodic responses in the high-frequency bands were detected similarly as for the low-frequency bands: (1) the FFT spectrum was cut into segments of 50 bins centered at the response frequencies (i.e., 1.2 Hz for the Face Localizer and Unfamiliar Face Discrimination paradigms, 0.666 Hz for Famous Face Identity) and harmonics, until the last harmonic before 6 Hz base frequency; (2) the amplitude values of these FFT segments were summed; (3) the summed FFT spectrum was transformed into a Z-score. A contact was considered as showing a significant response if the Z-score at the target frequency bin exceeded 3.1 (i.e., $p < 0.001$). The quantification of response amplitudes was done similarly as for the low-frequency bands (sum across harmonics followed by baseline-correction).

2.6. Cortical face-selective regions in fMRI

We localized face-selective regions in fMRI with a Fast Periodic Stimulation fMRI paradigm (Gao et al., 2018, see **Supplementary Information**). This approach is not only similar to the Face Localizer paradigm used in SEEG (Fig. 4), but identifies face-selective fMRI activity at typical locations of the VOTC (and superior temporal sulcus [STS]) with higher signal-to-noise ratio and internal reliability than conventional face localizers, while excluding contributions from low-level cues contained in the amplitude spectrum of the images (see Gao et al., 2018).

DN was tested with fMRI 7 months after the SEEG procedure. Natural non-face object images were presented at a fixed rate of 6 Hz (i.e., 6 images by second). Mini face “bursts” with a duration of 2.167 s were embedded at every 9 s (i.e., $1 / 9 = 0.111$ Hz). Each burst consisted of a set of seven natural face images interleaved with six object images, in order to avoid potential neural adaptations to consecutive face images. The face burst created direct contrast between face and non-face objects. Therefore, a neural response measured exactly at 0.111 Hz reflects a selective and reliable response to the face stimuli. Each fMRI sequence (run) lasted 333 s of 36 cycles of mini face burst appearing at every 9 s (including a 9 s baseline). DN was tested with six functional localizer runs. The whole testing session took about one hour, including breaks. To measure the magnitude of the face-selective responses at the stimulation frequency of 0.111 Hz, we extracted the amplitude spectrum from the preprocessed BOLD time series with a Fast Fourier Transform (FFT) (see **Supplementary Information**, and all methods as in Gao et al., 2018).

For result visualization, the functional activation map was coregistered to the high-resolution T1-weighted image (AC-PC plane aligned) using SPM (<https://www.fil.ion.ucl.ac.uk/spm/>). Cortical surface of DN’s brain was also reconstructed by segmenting the anatomical volumes into gray and white matter using *Freesurfer* (<https://surfer.nmr.mgh.harvard.edu/>, version 5.0). To assess the spatial relationship between face-selective activations and intracerebral electrodes, we further extracted the electrode contact coordinates by fusing the T1-weighted image with the post-operative CT-scan.

To examine whether some electrode contacts overlap with the fMRI signal drop-out area in the ventral ATL region, we mapped contacts onto the mean temporal signal-to-noise (tSNR; Krüger and Glover, 2001) ratio map across all six functional runs. The tSNR map was calculated in each voxel of each functional run (with no spatial smoothing) as the mean signal divided by the standard deviation of the time series. We also created disk ROIs with a radius of 1 mm centered on each contact of electrode TM and extracted the mean tSNR value across voxels in each contact ROI from the mean tSNR map. The mean tSNR map was also coregistered to the T1-weighted image.

3. Results

3.1. Overview of the experimental plan

In subject DN, intracerebral electrical stimulations were applied between two adjacent intracerebral contacts while he was tested with an original set of various tasks, including famous face, famous building, and visual object naming tasks, but most importantly, a famous face pointing task (and its famous name counterpart) and famous or unfamiliar face matching tasks that did not require any verbal output (Fig. 3A and 3B, respectively). Importantly, outside the SEEG procedure, DN’s performance on all these pointing/matching tasks was at ceiling (100% of accuracy on upright faces, **Supplementary Table 1**), so that every failed trial during the time of the electrical stimulation could be considered as a genuine impairment related to the stimulation.

Considering the limited amount of time afforded by the clinical context, we first identified the relevant electrode contacts for FIR with the famous face pointing task (which allows to test DN’s FIR ability without requiring any verbal output) and then further tested these contacts with the remaining tasks. Since we found a FIR impairment when stimulating the first electrode tested, i.e., electrode TM (Fig. 2A), we focused on this electrode to maximize the number of tasks and trials (consequently, other electrodes were not stimulated with face-related tasks). Independently of the electrical stimulation sessions, we identified face-selective contacts and contacts sensitive to unfamiliar face discrimination and famous FIR using well-validated FPVS paradigms during SEEG recordings (Fig. 4, see also **Supplementary Information** for all methods details), in both low- and high-frequency bands. Finally, we local-

ized face-selective regions in fMRI with a Fast Periodic Stimulation fMRI paradigm performed 7 months after the SEEG procedure.

3.2. Right AntFG and AntOTS stimulation elicits transient face identity recognition impairment

DN was transiently impaired at pointing out the famous face during electrical stimulation of contacts TM4-TM5 and TM5-TM6 in the right AntOTS (tested across 14 stimulation sessions) as well as contacts TM1-TM2 in the right AntFG, although this last site was stimulated only once (Talairach coordinates: $x: 31$ to 37 , $y: -21$, $z: -17$, Fig. 2A). DN failed at least one trial during the stimulation time for 11 out of 15 stimulation sessions involving these 3 sites (Supplementary Table 2). For these failed trials, DN either did not respond, or pointed to an unfamiliar face (Videos S1, S2 and S3). Across the 15 stimulation sessions involving these contacts, his performance was at ceiling before and after stimulation (70/70 trials succeeded, 100%). Critically, his performance dropped significantly during the time of stimulation (11/24, 45.8%, $\chi(1) = 44.002$, $p < 0.001$).

DN was fully aware of his transient difficulty at face identity recognition. During the stimulation, he stated for example: “I don’t know who he is”; when probed by the experimenter after stimulation, DN reported: “I don’t know the 3 faces you showed me”, “I had difficulties recognizing her”, “I looked at the 3 faces and I had a doubt”, “I didn’t recognize the face immediately” (Videos S1 and S3). When DN was presented with the trials in which he failed during stimulation (after 5 TM4-TM5 and 1 TM1-TM2 stimulation sessions) and asked to perform the task again, he quickly pointed to the famous faces without errors (8/8 trials) (for examples, see Videos S1 and S2). Importantly, DN never reported any face distortions. When asked explicitly if the face was distorted, he responded: “No, it wasn’t”, “No, not at all”.

It is important to note that for the 4 stimulation sessions of TM4-TM5 and TM5-TM6 contacts during which DN answered correctly for all trials, he was in fact hesitant when performing trials during stimulation. For these correctly responded trials across these 4 stimulation sessions, there was a significant increase of the response times during stimulation ($n = 6$, mean = $2420 \text{ ms} \pm 521.4 \text{ ms}$) compared to time periods outside stimulation (before: $n = 9$, mean = $1120 \text{ ms} \pm 175.5 \text{ ms}$; after: $n = 12$; $1113 \text{ ms} \pm 313.9 \text{ ms}$) ($F(2,24) = 35.391$, $p < 0.001$) (Fig. 5A). A post hoc Bonferroni test showed that correct response times during stimulation were significantly slower than correct response times before or after stimulation ($p < 0.001$ for both “before-during” and “during-after” comparisons). In agreement with these results, a Bayesian analysis (performed in JASP; see van Doorn et al., 2021 for the interpretation guidelines of BF values) showed extreme evidence for the alternative hypothesis with a Bayes Factor (BF10) equal to 111900.665, meaning that the data was 111900 times more likely to occur under the alternative hypothesis (i.e., there is a difference between testing times) than under the null hypothesis (i.e., there is no difference).

Stimulating electrode TM contacts outside these effective sites (TM2-TM3, TM3-TM4 in the AntCOS, TM6-TM7 in AntOTS, and TM7-TM8, TM8-TM9, TM9-TM10, TM10-TM11, TM11-TM12, TM12-TM13 in the anterior inferior temporal gyrus; Fig. 2A) did not evoke any mistakes or omissions at pointing out famous faces (100% of accuracy across 9 stimulation sessions: 39/39 trials outside stimulation, 20/20 trials during stimulation, Supplementary Table 2).

Subject DN was also tested with simultaneous unfamiliar and famous face matching tasks, which allow to specifically test face individuation and the integrity of facial percepts (with and without the help of long-term memory of specific identities). During stimulation of contacts TM4-TM5, DN was transiently impaired at matching unfamiliar and famous faces. With unfamiliar faces, he failed at least one trial during stimulation for 2 out of 2 stimulation sessions (i.e., pointing to the wrong face). For one stimulation session, he failed one trial during stimulation and for the second, he failed 3 trials during stimulation, and 2 after stimulation (Video S4). Across the 2 stimulation sessions, his per-

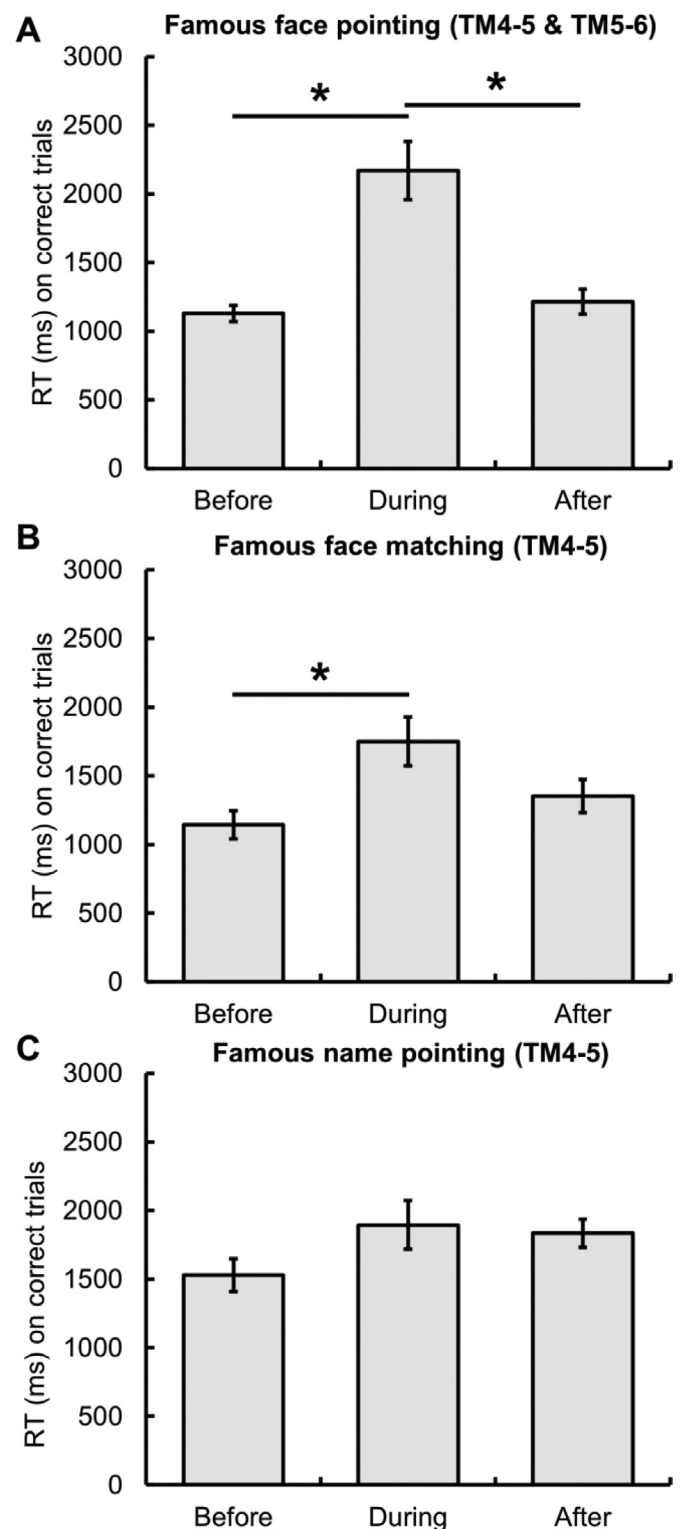


Fig. 5. Response times for correct trials before, during and after electrical stimulation of electrode TM contacts for the famous face pointing task, the famous face matching task and the famous name pointing tasks. A. Response times for the famous face pointing task before, during and after stimulation of contacts TM4-TM5 and TM5-TM6 (across 4 stimulation sessions without any failed trials). B. Response times for the famous face matching task before, during and after stimulation of contacts TM4-TM5 (across 2 stimulation sessions without any failed trials). C. Response times for the famous name pointing task before, during and after stimulation of contacts TM4-TM5 (across 7 stimulation sessions without any failed trials). Error bars indicate standard error. RT, response time; (*) indicates significant difference at $p < .001$.

formance was 100% before stimulation (4/4), 50% during stimulation (4/8, i.e., chance level) and 33% after stimulation (1/3). Accuracy did not statistically differ between stimulation and non-stimulation periods ($\chi(1) = 0.714$, $p = 0.398$) because the effect of the second stimulation lasted longer, decreasing his performance outside stimulation (5/7, 71%). When comparing the before and during stimulation time periods only, we found a trend towards a difference ($\chi(1) = 3$, $p = 0.083$), but not significant probably because of a low number of trials. Across 2 stimulation sessions with the famous face matching task, DN performed correctly at all trials presented outside (12/12) and during (4/4) stimulation. As for the famous face pointing task, we compared the correct response times during the famous face matching task for the three testing times (before, during and after). A one-way ANOVA highlighted a significant difference between testing times ($F(2,25) = 5.517$, $p = 0.018$) (Fig. 5B). More precisely, post-hoc tests showed that DN was significantly slower to answer the trials presented during stimulation ($n = 4$, mean = $1750 \text{ ms} \pm 356.8 \text{ ms}$) compared to those presented before stimulation ($n = 7$, mean = $1143 \text{ ms} \pm 268.2 \text{ ms}$) ($p = 0.017$). Response times after stimulation ($n = 5$, mean RT = $1352 \pm 270.4 \text{ ms}$) were not significantly different from response times in other testing periods. Bayesian analysis supported this effect by showing moderate evidence for the alternative analysis ($BF_{10} = 3.623$).

Although it does not allow to distinguish between naming and recognition impairments, we also asked DN to perform a famous face naming task when stimulating electrode TM (Supplementary Table 2) since this task led to FIR impairments in previous electrical stimulation studies (Puce et al., 1999; Jonas et al., 2012, 2015; see Jonas and Rossion, 2021). Electrical stimulation of TM4-TM5 in the right AntOTS (Fig. 2A) evoked a transient inability to name famous faces (2 out of 2 stimulation sessions). DN's performance was at 100% on trials outside stimulation (7/7 trials before, 7/7 after) but was reduced to 25% during electrical stimulation (1/4 trials; $\chi(1) = 12.600$, $p < 0.001$). Stimulation ($n = 1$) of TM5-TM6 did not impair famous face naming (2 trials during stimulation; Supplementary Table 2; see Supplementary Fig. S2 for response times).

In summary, electrical stimulation involving the right AntFG and adjacent AntOTS (bipolar stimulations on contacts TM1-TM2, TM4-TM5 and TM5-TM6, Table S2, Fig. 2A) of subject DN evoked a reliable transient FIR impairment expressed across a variety of behavioral tasks (famous face naming, pointing to a famous face among distractors, matching different views of famous or unfamiliar faces for identity), with contact TM5 being the most consistently effective (i.e., electrical stimulations involving contact pairs TM4-TM5 or TM5-TM6 most consistently elicited transient impairments, with failed trials in 10 out of 14 stimulation sessions with the famous face pointing task, Supplementary Table 2).

3.3. Specificity for faces

Although stimulation of the effective contacts TM4-TM5 evoked an inability to name famous faces, stimulation of this site did not affect naming of non-face objects. DN was able to name all pictures of visual objects (across 3 stimulation sessions: 9 objects during stimulation and 18 before or after stimulation) and all famous buildings (1 stimulation session: 2 famous buildings during stimulation and 6 outside stimulation). There was also no significant increase of the response times related to the stimulation for these two tasks (Supplementary Fig. S2).

Most importantly for the present investigation, we evaluated whether the identity recognition impairment was specific to the category of faces and not due to a general semantic impairment by assessing DN's ability to recognize written names of famous people. During 7 stimulation sessions of contacts TM4-TM5, DN performed a famous name pointing task (Fig. 3A), using the same procedure as the famous face pointing task (1 famous name and 2 unfamiliar phonologically-similar fictional names), a task that DN performed perfectly during his neuropsychological evaluation outside the SEEG procedure (Sup-

plementary Table 1). There was no impairment at all at this task, DN being flawless across the 7 stimulation sessions (17 trials during the stimulation, 34 trials before or after stimulation). Moreover, there were no differences in response times between trials outside stimulations (before: $n = 18$, mean = $1528.3 \text{ ms} \pm 505.6 \text{ ms}$; after: $n = 16$; $1835 \text{ ms} \pm 420.8 \text{ ms}$) and trials during stimulation ($n = 17$, mean = $1894.1 \text{ ms} \pm 730.5 \text{ ms}$, Fig. 5C). There was no statistical difference between testing times, i.e., before, during and after ($F(2,48) = 2.089$, $p = 0.135$). Concordantly, Bayesian analysis showed anecdotal evidence for the null hypothesis ($BF_{10} = 0.672$).

3.4. Visual memory impairment following stimulation

Immediately after 15 stimulation sessions out of 21 involving FIR tasks (famous face naming, famous face pointing, unfamiliar and famous face matching task), DN was presented again with some of the trials (i.e., single faces or triplets) presented during the stimulation and was asked to indicate verbally if they had been presented during the stimulation session (15 stimulation sessions: 9 with impairment and 6 without; 14 of contacts TM4-5 and 1 of contacts TM5-TM6). Across these 15 stimulation sessions, DN did not remember 16 out of 21 trials presented during stimulation (23.8% of accuracy, 13 stimulation sessions with at least one non-remembered trial). For these non-remembered trials, when asked if he just saw one of the trials presented few seconds before, DN answered "no" (Videos S1 and S2). In contrast, he correctly remembered having seen 24 out of 24 trials presented outside stimulation, before or after (100% accuracy). This difference was significant ($\chi(1) = 28.37$, $p < 0.001$). Outside stimulation, he also correctly detected 15 out of 15 distractor faces (100% accuracy).

Interestingly, although he was never impaired at recognizing non-face stimuli during stimulation, his difficulty to remember trials presented during the stimulation extended to all stimuli, not just faces (Video S5). Across 2 stimulation sessions with the object naming task, he was unable to remember 4 out of 7 objects (42.8% of accuracy) presented during stimulation, while he correctly remembered all 5 objects presented outside the stimulation and correctly detected 2 distractors. For the famous building naming task, he was unable to remember 1 building presented during stimulation, but correctly remembered 3 out of 3 buildings presented outside the stimulation and correctly detected the only distractor presented. Across 7 stimulation sessions with the famous name pointing task, he was unable to remember 8 out of 17 trials presented during stimulation (47% of accuracy), while he correctly remembered 16 out of 16 names presented outside the stimulation and correctly detected 4 out of 4 distractors.

In summary, while the transient identity recognition impairment during electrical stimulation appeared only during face tasks, the subsequent difficulty to remember which items were presented during the stimulation was found regardless of the stimulus category.

3.5. Face-selectivity of effective contacts

To localize the effective contacts with respect to the cortical face network, DN was tested (7 months after the SEEG procedure) with a Fast Periodic Stimulation fMRI paradigm (Gao et al., 2018). Fig. 6 shows the face-selective clusters at a threshold of $p < 0.001$ (uncorrected; z -score > 3.1), with a minimal cluster size of $10 \times 2.5 \times 2.5 \times 2.5$ voxels (see also Supplementary Table 3). Face-selective fMRI activity in DN was strongly right lateralized and concerned the typical cortical face network, with two significant face-selective clusters in the lateral part of the posterior/middle right FG (pFG and mFG), corresponding to the well-known "FFA" (Kanwisher et al., 1997) or pFus and mFus-faces (Weiner and Grill-Spector, 2012a). Other clusters were located in the right posterior STS (right pSTS), and in the lateral part of the posterior left FG (left pFG).

Fig. 6A to D show that the critical electrode contacts whose stimulation led to transient impairment at recognizing the identity of faces

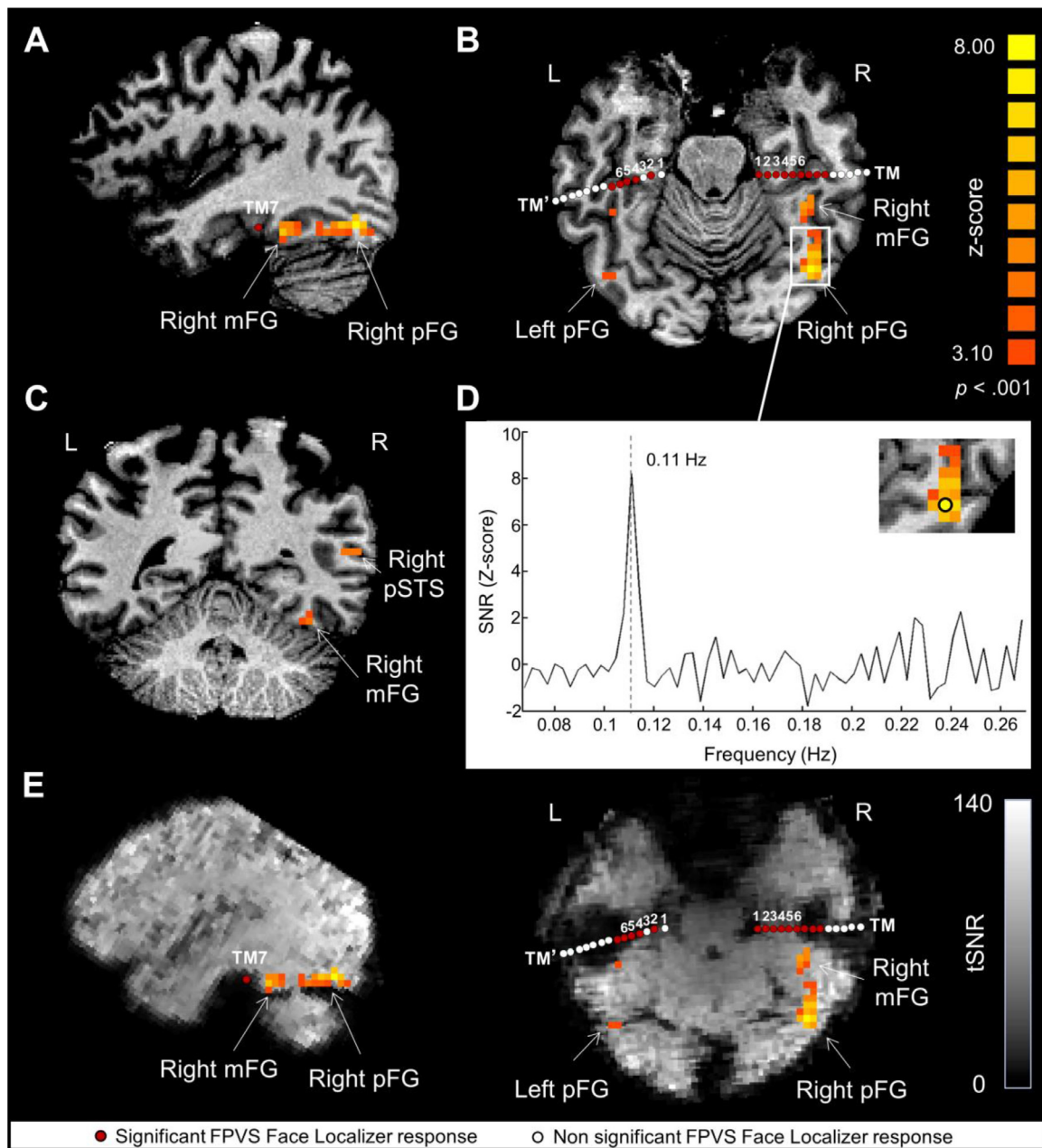


Fig. 6. The critical stimulation sites eliciting transient impairment at recognizing facial identities are located anteriorly to the middle fusiform face-selective clusters identified by fMRI and at the edge of the fMRI signal drop-out. A. Sagittal slice passing through contact TM7 (red dot). B. Axial slice passing through electrode TM. Red and white dots represent contacts of electrodes TM and TM', colored according to their face-selectivity with the FPVS/SEEG Face Localizer paradigm in the low-frequency bands. C. Coronal slice passing through right pSTS and mFG face-selective clusters. D. SNR spectrum at the face stimulation rate (i.e., 0.11 Hz) of the peak voxel in the right pFG (highlighted by a black circle). E. Superimposition of the fMRI face-selective clusters and electrodes TM and TM' (red and white dots) in sagittal (left) and axial slices (right) onto the mean tSNR map. The critical stimulation sites on electrode TM are located at the edge of a strong fMRI signal drop-out. mFG, middle fusiform gyrus; pFG, posterior fusiform gyrus; pSTS, posterior superior temporal sulcus.

(i.e., TM1, 2, 4, 5 and 6) were located anteriorly to the right mFG cluster, i.e., right “FFA” (see also Fig. 7A for an inflated cortical surface map). There was no overlap between the significant face-selective clusters and the critical contacts, even when the functional activation clusters were defined with a relatively liberal threshold of $p < 0.05$, uncorrected.

It is widely known that the fMRI signal drops out significantly in the ventral ATL in echo-planar imaging due to field gradient distortions from magnetic susceptibility differences between air/tissue and bone/tissue interfaces (Wandell, 2011; Axelrod and Yovel, 2013; Rossion et al., 2018). This might explain why we found no face-selective

activations in the right AntFG, where the critical contacts were located. To test this assumption, we measured the mean tSNR ratio across the six functional runs and overlaid the electrode TM and TM' contacts on top of it (Figs. 6E and 7B). As expected, the critical TM contacts were located at the edge of a severe signal loss in the right ventral ATL, according to the tSNR thresholds reported in previous studies (e.g., Friedman et al., 2006; Murphy et al., 2007), with the tSNR values ranging between 9 and 38 (e.g., TM1: 9, TM2: 25, TM3: 32, TM4: 38, TM5: 38, TM6: 27). Instead, an equal-sized ROI defined in the right mFG region including the peak face-selective activity had a larger tSNR value at 65. Moreover, no face-selective clusters were found in the AntFG, as if the right mFG

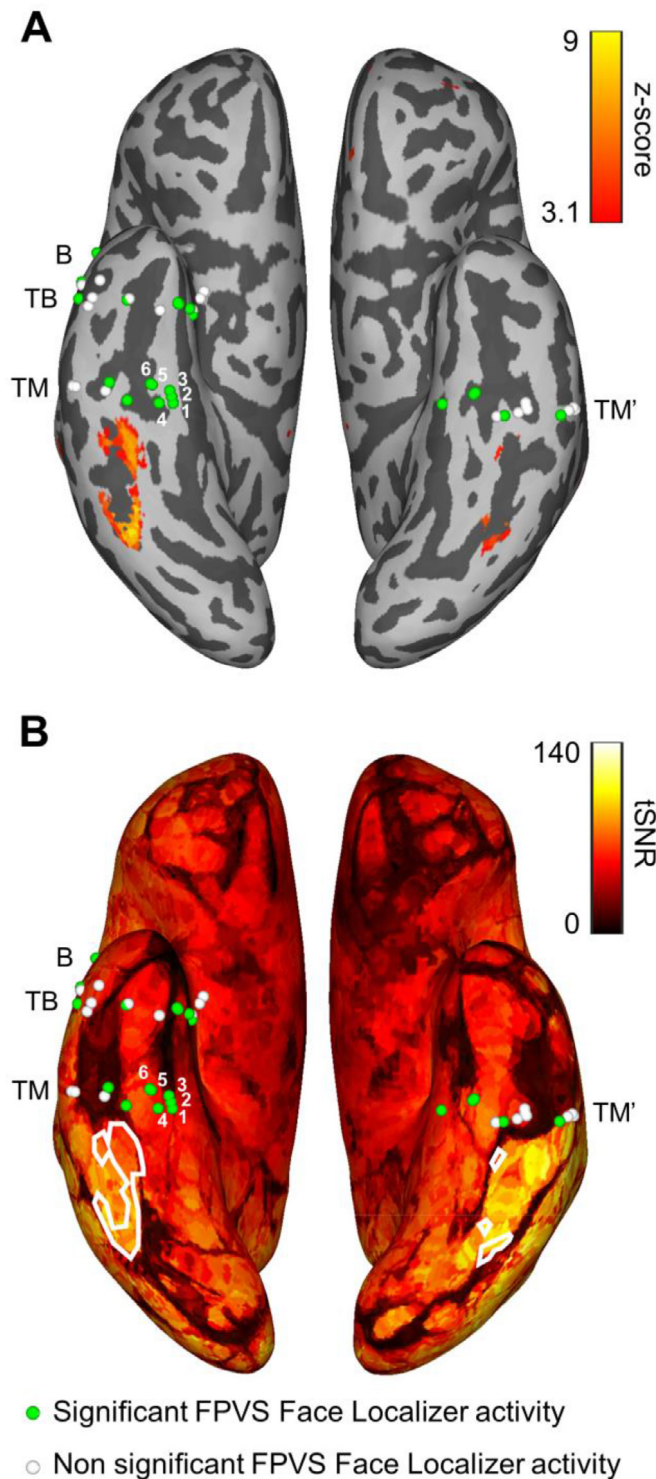


Fig. 7. Face-selective activations, tSNR and intracerebral contacts mapped onto the inflated cortical surface of DN's brain. **A.** Ventral view of fMRI face-selective activations in the VOTC. Contacts of electrodes TM, TB, B and TM' are displayed through green or white circles, colored according to their face-selectivity with the FPVS/SEEG Face Localizer paradigm in the low-frequency bands. Some TM contacts, including the effective contacts are labeled (1 to 6). Note that the inflation process spreads contacts on both sides of the sulci, disrupting the initial linear arrangement of SEEG electrodes. **B.** Superimposition of the fMRI face-selective activations in the left and right VOTC (white outlines) and electrodes TM, TB, B and TM' (green and white dots) onto the mean tSNR map.

cluster was cut short, anteriorly, by the signal drop-out (Figs. 6E and 7B).

We also measured electrophysiological face-selective responses on each contact in both low-frequency and high-frequency bands with a validated face-localizer FPVS paradigm during SEEG recordings (Jonas et al., 2016; Hagen et al., 2020; Fig. 4A). Despite the lack of face-selective response in fMRI, highly significant frequency-tagged face-selective responses occurring exactly at 1.2 Hz and harmonics were found on contacts TM1 to TM9 in the low-frequency bands (Fig. 2B). Impressively, among all contacts of electrode TM but also among all 141 contacts implanted in DN's brain, the largest face-selective response amplitude was found on the effective contact TM5 (Fig. 2B; see also Supplementary Fig. S3). Significant face-selective responses were also found on 17 other contacts outside electrode TM in the left and right ATL (Fig. 8).

Face-selective periodic bursts of high-frequency broadband activity (30 to 160 Hz) at 1.2 Hz (see Materials and methods) were also found on several contacts of electrode TM (Fig. 2B), including the effective contacts TM1, TM2, TM4, TM5, TM6, and with a maximum amplitude on TM5 (Fig. 2B; see also Supplementary Fig. S3). Fig. 9 shows these bursts of face-selective high-frequency activity following the face presentation recorded on TM5 as they appear in the time-frequency analysis, as well as a time-domain analysis of the face-selective high-frequency activity on this contact, with an onset time estimated around 130 ms. Two significant high-frequency band responses were also found in the left ATL (Fig. 8).

In summary, both the largest face-selective responses in low- and high-frequency bands were found on contacts whose stimulation elicited a transient FIR impairment, and the highest face-selective amplitude was found on the effective contact TM5.

3.6. Sensitivity of effective contacts to unfamiliar and famous face identity

Finally, we tested sensitivity to face identity on each intracerebral contact independently of the electrical stimulation with two FPVS paradigms.

First, we tested sensitivity to unfamiliar face discrimination, i.e., sensitivity to discriminate face identity based on the visual information that makes a face unique independently of long-term memory, with a paradigm that periodically introduces different unfamiliar face identities among a train of same-identity face stimuli (Liu-Shuang et al., 2014; review in Rossion et al., 2020; Fig. 4B). We found significant unfamiliar face discrimination responses in the low-frequency bands for the upright face condition on contacts TM1, TM4, TM5 and TM6 (Fig. 2C). There was no significant response on any other implanted contacts (Fig. 8). Among all recording contacts, the amplitude was again the largest on contact TM5 (Fig. 2C; see also Supplementary Fig. S3). This experiment was also performed with inverted faces, allowing to isolate neural indexes of face individuation that go beyond physical differences between images. There was no significant response on electrode TM, or on any other electrodes for inverted faces (except on one contact in the left hemisphere). We found a significant difference between upright and inverted conditions on contacts TM4 and TM5 only with, again, the largest amplitude difference found on TM5 among all contacts (see Supplementary Fig. S3). In high-frequency bands, an unfamiliar face discrimination response was found only on contact TM1, only for upright faces (Fig. 8). Second, we also tested sensitivity to famous FIR on each intracerebral contact using a FPVS paradigm contrasting famous and unfamiliar faces in which different face exemplars of the same famous identity are presented periodically in a fast periodic train of variable unfamiliar faces (Fig. 4C; Zimmermann et al., 2019; Yan et al., 2020). In this experiment, we recorded robust responses in the low-frequency bands exactly at the famous face identity frequency on contacts TM1, and from TM3 to TM7 (Fig. 2D), with the largest response again recorded on TM5 among all contacts implanted in DN's brain (Fig. 2D, see also Supplementary Fig. S3). Significant responses were also found on 4 contacts in the left

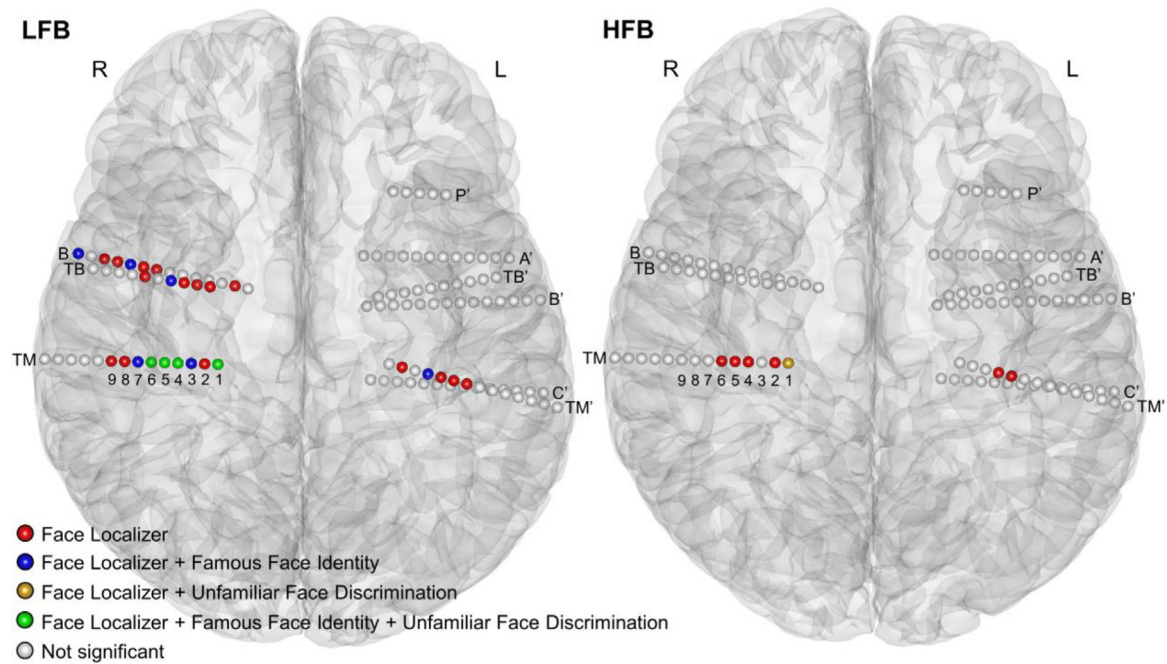


Fig. 8. Spatial distribution of SEEG electrodes in DN's VOTC and significant responses to three FPVS experiments (Face Localizer, Unfamiliar Face Discrimination [upright condition] and Famous Face Identity [upright condition]) in the low-frequency bands (LFB, left panel) and high-frequency bands (HFB, right panel). Intracerebral contacts are plotted in the native MRI space using a transparent reconstructed cortical surface of DN's brain (ventral view). Each circle represents a single intracerebral contact. White-filled circles represent contacts with no significant response. Colored circles represent contacts with one or several significant responses across the 3 FPVS experiments. For visualization purposes, individual contacts are displayed larger than their actual size (2 mm in length). Electrodes' names are displayed on the outer side of each electrode.

and right ATL (Fig. 8). For inverted faces, response amplitudes at the famous face identity frequency were much weaker than in the upright condition on electrode TM (Fig. 2D). The difference between upright and inverted conditions was significant on contacts TM1, and from TM4 to TM7 ($p < 0.001$), with the largest amplitude difference found on TM5 among all recorded contacts (Fig. 2D; Supplementary Fig. S3). A significant difference between upright and inverted conditions was also found on 3 right-lateralized contacts (contacts TB4, B10 and B12) and 3 left-lateralized contacts (contacts TM'4, TM'5, and A'9, see Fig. 8 for contact location). In high-frequency bands, no response was significant in the upright condition.

4. Discussion

4.1. Contextual summary of the present observations

By electrically stimulating a face-selective region in the right AntFG and adjacent AntOTS (contacts TM1-TM2, TM4-TM5, and TM5-TM6), we evoked a transient inability to recognize the identity of faces. Some of the findings reported here are similar to a previous stimulation case study of the same region (subject CD, Jonas et al., 2015). In both cases: (1) the effective stimulation site was located in the right AntFG and adjacent AntOTS, anteriorly to the right FFA or mFG; (2) the stimulation of this effective site elicited a transient inability to recognize famous faces; (3) this effect was specific to faces, with no recognition impairment being observed for non-face stimuli; (4) the impairment at recognizing famous faces was not associated with visual distortions of perceived faces; (5) a difficulty to remember which visual items were presented during the stimulation, not specific to faces, was almost systematically present; (6) the stimulation site was shown as face-selective in low-frequency and high-frequency bands but not in fMRI, since it was located in a severe signal drop-out affecting this region.

Despite these striking similarities, the present study goes well beyond the previous case report of Jonas et al. (2015). First, outside the stimulation procedure, subject CD already presented difficulties at recognizing famous faces. In contrast, subject DN reported here performed extremely well with famous faces (100% accuracy at the famous face pointing task performed outside the SEEG procedure). Second, during electrical stimulation, subject CD was tested only with a face task requiring a verbal output (naming famous faces). In order to ensure that the deficit was not due to naming access/output (as potentially in a number of early cases of face naming impairment following intracranial stimulation, often of the left VOTC, Allison et al., 1994; Puce et al., 1999; see Jonas and Rossion, 2021), DN was stringently tested here with a famous face pointing task. Third, we were able to perform an unusually large number of stimulations and trials (15 stimulation sessions of the effective sites with the famous face pointing task, i.e., 97 trials including 27 trials during stimulation) in the present case. This allowed us to reliably quantify and statistically test the effect of stimulation, both in accuracy (drop from 70/70 trials succeeded outside stimulation i.e., 100%, to 11/27 during stimulation, i.e., 45.8%) and in correct response times (increase of mean response time from 1116 ms outside stimulation to 2420 ms during stimulation of the effective contacts; i.e., 117% increase). Fourth, DN was uniquely tested with a wide range of face tasks, including two face tasks with their non-face counterparts (i.e., famous face and famous building naming tasks, famous face and famous name pointing tasks), allowing to assess the face specificity of the observed effect. Upon stimulation of the very same contacts inducing a transient FIR deficit, there were no errors or increased response times for the non-face tasks. Moreover, DN was tested with a simultaneous face matching task (unfamiliar and famous) allowing to specifically test face individuation independently of his long-term and short-term memory of specific facial identities. When stimulating the effective contacts, DN was impaired at this task.

Beside being able to find the famous written name among two distractors and rapidly name famous buildings in similar tasks failed for

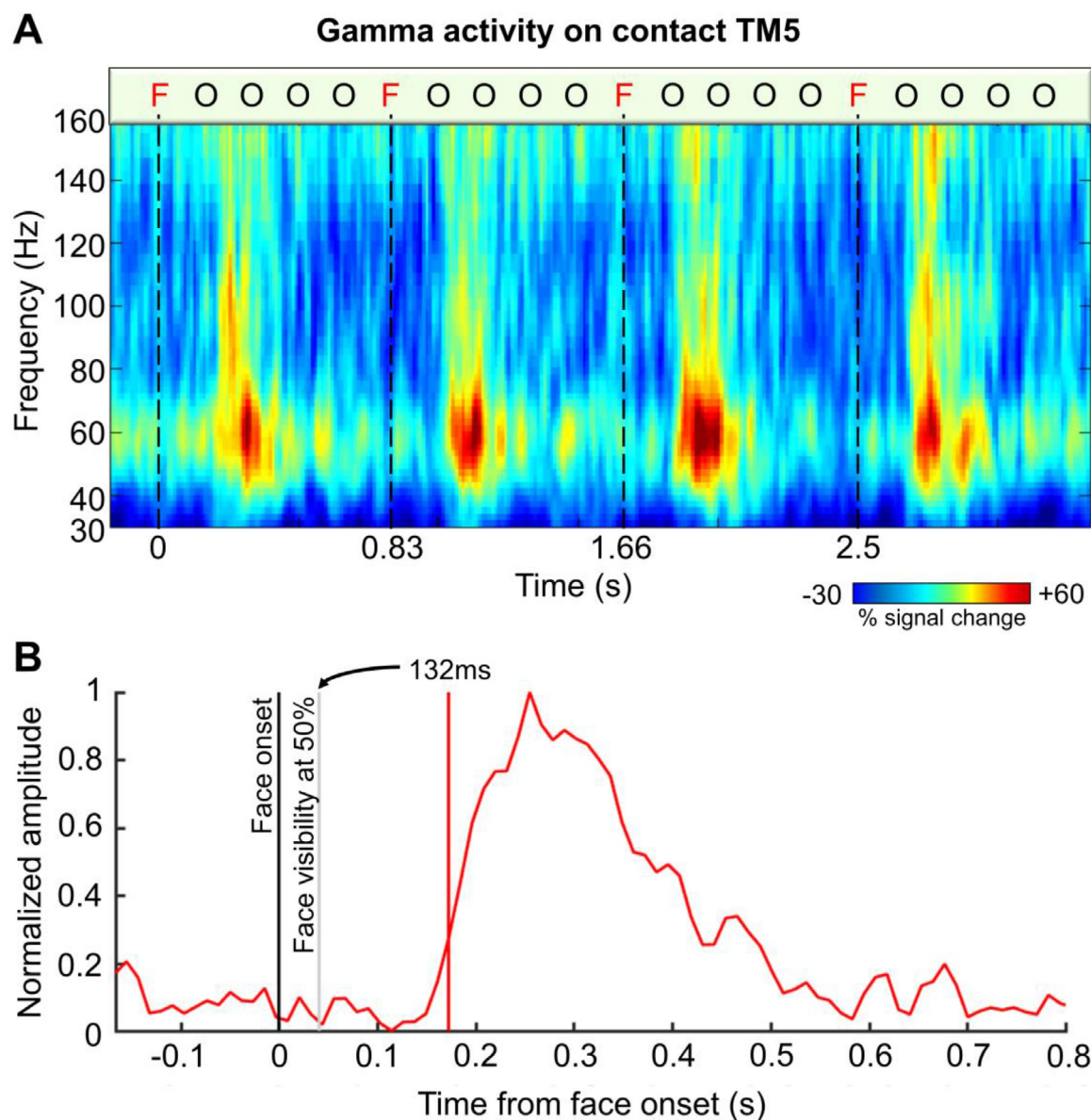


Fig. 9. Broadband high frequency (gamma activity) recorded on contact TM5. **A.** Time-frequency analysis of high-frequency bands recorded on contact TM5 during the Face Localizer frequency-tagging experiment (obtained after averaging the 4 Face Localizer sequences recorded in DN [66 s each, without fade-in and fade-out], segmenting the average segment into 19 epochs containing 4 face cycles each, and then averaging these epochs). Gamma activity occurs between 30 Hz and 120 Hz but with a larger response centered around 60 Hz. This response is largely increased following the periodic presentation of the faces. These periodic bursts of gamma activity are captured in the frequency-domain analysis shown in Fig. 2B. F: Face; O: Object. **B.** Time-domain analysis of the high-frequency response displayed in A. Signal related to the 6 Hz base frequency and its harmonics was filtered out. Face Localizer sequences were segmented relative to each face onset (i.e., every 0.83 s, to extract 1 face cycle), and resulting epochs were averaged. The black line indicates the onset of face presentation. The red vertical line shows estimated onset latency of face-selective responses in the high-frequency bands (i.e., computed as the time-point at which the SEEG response exceeded ± 2.58 times the standard deviation of the amplitude in the interval before the face onset [-0.166 to 0s], $p < 0.01$, two-tailed, for at least 30 ms). As stimuli appeared through sinusoidal contrast modulation, the corrected face onset time is indicated with a grey line, shifted forward from the black line by 41 ms (i.e., $\sim 1/4$ of a 6 Hz cycle duration, corresponding to a face contrast of about 50% of the maximal; Retter and Rossion, 2016). After correction, the onset latency of face-selective responses in the high-frequency bands was thus estimated to 132 ms.

faces when stimulating the very same effective contacts, DN was also able to name visual non-face objects. Thus, the recognition impairment due to stimulation appeared to be specific to faces (i.e., transient prosopagnosia). Admittedly, due to the constraints of the clinical setting (i.e., limitations in the number of stimulation trials and overall testing time), we did not test DN with more challenging tasks for non-face items, requiring recognition of unique entities (beyond famous buildings) or within-category recognition/discrimination for instance. While this would have undoubtedly constituted additional control tasks to ensure specificity of the recognition impairment to faces, it would

have reduced the number of trials and diversity of the tasks performed with the latter stimuli, which we prioritized in this investigation. Moreover, it is important to stress that brain-damaged patients who have increased difficulties at matching/discriminating pictures of visually similar non-face objects are cases of visual agnosia rather than prosopagnosia, and therefore, unlike DN, also always present difficulties even at simple basic-level visual object recognition (e.g., Levine and Calvanio, 1989; Gauthier et al., 1999; see Rossion, 2018 for a rebuttal of the within-category discrimination account of prosopagnosia).

As a final original contribution as compared to the previous case report with effective stimulation in the right AntFG, a FPVS approach providing objective and highly sensitive neural responses to identify and quantify the face-selectivity and the sensitivity to unfamiliar face discrimination and famous face identity at the effective stimulation sites was introduced in the present case. With this approach, we found that all effective contacts associated with face recognition impairments when stimulated were face-selective in both low- and high-frequency bands (TM1, TM2, TM4, TM5, TM6), with the highest amplitudes among all recorded contacts in DN's brain found on the consistently effective contact (TM5). Similarly, and strikingly, all effective contacts recorded unfamiliar face discrimination and famous face identity responses, with the largest amplitude in the upright condition and the largest amplitude difference between upright and inverted conditions found on TM5 again.

Altogether, these observations provide unique evidence that the right AntFG is a key node of the face-selective network, crucially involved in FIR. This observation is consistent with a study on low performers at recognizing faces without neurological history (i.e., prosopagnosia) who showed a volume reduction of their bilateral AntFG correlated with their behavioral decrement in famous face recognition (Behrmann et al., 2007). A similar observation has been reported in patients with fronto-temporal lobar degeneration (temporal and frontal variants), with a specific correlation with the right AntFG (Omar et al., 2011).

4.2. Where is the right AntFG region critical for face recognition located?

While the right AntFG highlighted here may be a critical node of the face-selective network, very little is known about its localization (and its functional role, see below), mostly because reliable BOLD activation is difficult to measure in this region due to a large signal drop-out arising from magnetic susceptibility artefacts (Wandell, 2011; Rossion et al., 2018; Fig. 1B). This SNR drop-out explains why only a fraction of fMRI studies report face-selective activity in this region (e.g., Nasr and Tootell, 2012; Rossion et al., 2012; Pyles et al., 2013) and why fMRI studies have usually reported a gap between the FFA and very anterior ATL activations close to the temporal pole (Fig. 1C). Using conventional fMRI sequences, we also failed to record face-selective fMRI activity in the right AntFG and around the critical sites of stimulation (TM1, TM2, TM4, TM5, TM6) of subject DN, despite the recording of strong face-selective FPVS/SEEG responses in low- and high-frequency bands on these contacts. Electrode TM was located at the heart of the signal drop-out created by magnetic susceptibility, with effective sites located at the edge of this no-signal zone. On these critical contacts, only a small fraction of the maximal fMRI signal was captured (tSNR range between 9 and 38). The recording of face-selective responses in this region in DN is, however, fully consistent with FPVS/SEEG group studies using the same paradigm and reporting large face-selective responses in the AntFG and AntOTS across many subjects (Jonas et al., 2016; Hagen et al., 2020).

The FG is divided into posterior and anterior parts by a coronal plane at the level of the posterior tip of the hippocampus (Onitsuka et al., 2003; Jonas et al., 2016) or at the level of the cingulate isthmus and splenium of the corpus callosum (Chau et al., 2014). The AntFG extends anteriorly up to the temporal pole. However, it is important to note that the right AntFG region critical for FIR highlighted in the present study and previously (subject CD; Jonas et al., 2015) extends only over a restricted part of the right AntFG, i.e., its most posterior part (Fig. 1A). This critical region is located just anteriorly to the posterior/anterior division of the FG and anterior to the FFA. The *y* Talairach coordinates of the critical contacts in subjects DN and CD were -21 and -30, respectively. Along the medio-lateral axis, the critical contacts are located both in the AntFG and its adjacent lateral sulcus, the AntOTS. The *x* Talairach coordinates of the critical contacts were 31 to 37 and 29 to 45 for subjects DN and CD, respectively. Therefore, although this region is often named "AntFG", critical face contacts are spread across two anatomical regions: the AntFG and the AntOTS. The involvement of the AntOTS

is particularly important to highlight since the effective contacts during electrical stimulation with the highest face-selective, unfamiliar face discrimination and famous face identity responses in DN, were located in fact in the AntOTS (stimulations on TM4-TM5 and TM5-TM6). As such, these two anatomical structures may belong to a single functional and cytoarchitectonic area, as it is the case most posteriorly in the middle FG where the lateral part of the FG and the adjacent OTS belong to the same face-selective region (i.e., the FFA, Kanwisher et al., 1997; Weiner and Grill-Spector, 2012) and to the same cytoarchitectonic areas (FG2 and FG4 along the posterior-anterior axis, Caspers et al., 2013; Lorenz et al., 2017). For sake of simplicity, we will henceforth refer to this region (face-selective posterior parts of the AntFG and AntOTS, critical for face recognition) as the AntFG face region.

4.3. What is the role of the right AntFG face region?

Keeping in mind that the effects of focal intracerebral electrical stimulation are not limited to the stimulation site of interest but may disrupt the function of directly connected regions or even putatively an entire network (Penfield, 1958; Borchers et al., 2012; Desmurget et al., 2013), at least three putative functional roles in face recognition could be attributed to the right AntFG face region. Given its relative anterior location in the VOTC and given that its focal stimulation reproducibly affected the recognition of famous faces, this region may play a role in multimodal person-recognition (Joubert et al., 2006; Gainotti, 2007; Blank et al., 2014) or in retrieving memories of familiar facial identities (Facial Recognition Units, FRU, Bruce and Young, 1986). However, recognizing familiar people based on their faces also requires extracting idiosyncratic features of these faces so that the right AntFG face region could also play a role in visual face individuation (independently of long-term familiarity).

Considering the visual memory impairment for the presented faces and the reported absence of perceptual face distortion, it may be tempting to interpret this face recognition impairment as a form of "associative prosopagnosia" through a disruption of the FRU (De Renzi et al., 1991; Davies-Thompson et al., 2014). Following this hypothesis, the stimulation would have transiently disconnected intact facial percepts and facial identity memory stores (FRU) or led to a transient loss of these facial memory stores. However, this hypothesis is unlikely to be correct, for several reasons. First, as for the previously reported case CD (Jonas et al., 2015), the difficulty to remember the specific items presented during stimulation was observed for all presented stimuli. This observation suggests that this form of post-stimulation amnesia, which may or may not be limited to visual items, is independent of the face-specific recognition impairment elicited in DN during stimulation. Instead, we hypothesize that this general visual memory impairment is due to a transient inactivation of the medial temporal lobe (MTL), in particular the hippocampus and rhinal cortex, so that the episode, i.e., here the (visual) stimuli presented during stimulation, cannot be encoded (Jonas and Rossion, 2021). That is, electrical stimulation of a highly modality- and category-specific region of the right AntFG does not only interfere with this region's function, but would also transiently disrupt the function of directly (i.e., monosynaptically) connected brain regions (Penfield, 1975; Borchers et al., 2012), in this case a MTL region that is critical in learning and category-general memory encoding (Dickerson and Eichenbaum, 2010; Jensen and Squire, 2012). This hypothesis is supported by clear stimulation artifacts recorded in both left and right hippocampi during right AntFG stimulation. It is also supported by studies showing that the AntFG is highly, directly, connected with the MTL memory system (hippocampus and rhinal cortex, Kahn et al., 2008; Catenoix et al., 2011; Libby et al., 2012; Zhang et al., 2016). In particular, a SEEG study exploring the connectivity of the hippocampus using cortico-cortical evoked potentials identified the AntFG ("ant T4") as one of the brain regions most highly connected to the hippocampus (Catenoix et al., 2011). Since the MTL function in memory encoding is generic rather than organized according to specific categories,

an interference at this level would extend to all types of presented stimuli, at least in the visual modality. Second, while the absence of visual distortion when stimulating the right AntFG (both in the present case DN and in the previously reported case CD) contrasts with stimulations performed in more posterior face-selective regions, i.e., right OFA and FFA, usually associated with conscious changes of the facial percept (facial elements in disarray, Jonas et al., 2012, facial palinopsia, Jonas et al., 2018; prosopometamorphopsia, Parvizi et al., 2012; Rangarajan et al., 2014), brain-damaged prosopagnosic patients who have clear unfamiliar face discrimination impairments do not experience perceptual distortions. Therefore, this contrast between the effects observed when stimulating the (right) AntFG and posterior face-selective regions could rather be explained by differences in their pattern of connectivity, with only the latter regions being directly connected with visual low-level (i.e., topographical) areas in the occipital lobe (Gschwind et al., 2012; Weiner and Zilles, 2016; Maher et al., 2019; Finzi et al., 2021; see Jonas and Rossion, 2021). Third, stimulating the right AntFG face region elicited a transient impairment at matching simultaneously presented pictures of faces for their identity, including (and even more so for) unfamiliar faces. This last observation provides direct evidence that DN's perception of facial identity was impaired, independently of short- and long-term memories of specific identities. Finally, the conceptual distinction between (visual) perception and memory impairments in patients with prosopagnosia is not clear-cut (Farah, 1990; Rossion, 2014). That is, so-called cases of "pure" associative prosopagnosia usually perform below normal range at matching different pictures of unfamiliar faces or rely on extremely slow and painstaking strategies (e.g., Levine and Calvanio, 1989; Davidoff and Landis, 1990; Farah, 1990; Delvenne et al., 2004). Moreover, most patients with right ATL lesions initially considered as "associative prosopagnosia" in fact show multimodal person recognition deficit affecting both face and voice identity recognition (e.g., Sergent and Poncet, 1990; Gainotti and Marra, 2011; see Gainotti, 2013a for review).

Based on these considerations, we would like to argue here instead that the right AntFG face region plays a critical role in *individuation*, both for familiar and unfamiliar faces, based primarily on indirect visual inputs (i.e., visual inputs that do not come from direct connections with the early visual cortex, unlike for the FFA and OFA; see Finzi et al., 2021). This interpretation is supported by several observations. First, as mentioned above, DN was impaired at matching simultaneously presented unfamiliar faces for their identity when stimulating this region, a task that was trivial for him during the neuropsychological assessment (Supplementary Table 1). Second, contacts evoking transient FIR impairments recorded large FPVS unfamiliar face discrimination responses and a recent SEEG group study with the same FPVS paradigm showed that the right AntFG is among the main regions supporting this function (Jacques et al., 2020). More specifically, in that study, unfamiliar face discrimination was found to be supported by a strip of cortex in the right VOTC including the right inferior occipital gyrus and the right middle FG, with an extension about 3 cm in the ATL along the right AntFG (y Talairach coordinates from -40 to -7), in the same region where subjects DN and CD were stimulated (y Talairach coordinates: -21 and -30, respectively). Strikingly, despite extensive sampling of the whole ATL up to the temporal pole, face identity discrimination responses were weak and rare in the remaining parts of the ATL, i.e., anteriorly to the AntFG region highlighted here, suggesting that the posterior section of the AntFG in the ATL supports unfamiliar face discrimination while the more anterior section of the ATL may rather be involved in the association of semantic information with specific face identities.

Finally, an outstanding issue is whether the right AntFG constitutes a modality- and category-selective region or rather a multimodal region involved in person-recognition (person semantic knowledge). On the one hand, a face-specific region is supported by several sources of evidence. First, as discussed above, the right AntFG is involved in visual face discrimination, a function rather dedicated to a modality-selective region. Second, during stimulation of the right AntFG face region, sub-

ject DN was not impaired at recognizing famous persons by their written names. Admittedly, this last control condition (famous name pointing) may not be optimal to assess the semantic functions of the right ATL. Indeed, verbal (name) and nonverbal (face and voice) person-specific information may be processed (relatively more) respectively in the left and right ATL (Gainotti, 2007, 2013b, 2015; Snowden et al., 2012, 2018; but see Rice et al., 2015, 2018; Hoffman and Lambon Ralph, 2018) so that right ATL lesions may lead to multimodal deficits for famous person recognition through face and voice inputs rather than (visual or auditory) names (Gainotti et al., 2003; Busigny et al., 2009; Hailstone et al., 2011; Gainotti 2013a; Cosseddu et al., 2018; but see Joubert et al., 2006 for a case of right ATL atrophy presenting with a multimodal person-based impairment affecting names in addition to faces and voices). Therefore, to fully assess the face-specificity of this region, one could test person recognition with another nonverbal modality, i.e., voice recognition, while applying electrical stimulation. Note that from a technical standpoint, this would be particularly challenging because voice identity recognition is far from being as accurate, automatic and fast as face identity recognition (Barsics, 2014; Lavan et al., 2016, 2019; Krix et al., 2017; see Young et al., 2020 for a recent review comparing human face and voice recognition). Third, a recent fMRI connectivity study focusing on the ATL showed that the AntFG is preferentially connected to the posterior face-selective regions (OFA and FFA) as a domain-specific region would be, and does not show a widespread connectivity with different modality-specific regions as it would have been expected if the AntFG was part of a cross-modal semantic hub (Persichetti et al., 2021).

On the other hand, the right AntFG face region might well be a multimodal region involved in person-recognition. Studies of patients with semantic dementia with a specific interest on the respective role of ATL subregions have shown that both the left and right AntFG play a role in semantics (Binney et al., 2010; Mion et al., 2010; Chen et al., 2019). Despite their methodological limitations to explore the ATL activity, some fMRI studies using distortion-corrected spin-echo protocol that enhances signal in the ATL reported activations for semantic tasks in the left and right AntFG (Binney et al., 2010; Visser et al., 2010, 2012; Visser and Lambon Ralph, 2011). Several sources of evidence (lesion and fMRI studies) also support the view that both left and right ATL may form a multimodal hub for person-identity recognition (Blank et al., 2014; Rice et al., 2018). One study of specific interest investigated the role of different ATL subregions in multimodal person recognition and found a correlation between grey matter volume in the right AntFG and voice to face-name cross-modal matching in both semantic dementia and Alzheimer's disease (Hailstone et al., 2011). However, the AntFG regions highlighted in these aforementioned lesion and fMRI studies were usually located more anteriorly than the right AntFG face region identified in the present study (e.g., y MNI coordinate: $y = -9$ in Binney et al., 2010; $y = -10$ in Mion et al., 2010; y between -8 and -20 in Visser et al., 2010; y between -15 and -17 in Hailstone et al., 2011; $y = -6$ in Chen et al., 2019; compared to y MNI coordinate of patients CD and DN, at -32 and -22 , respectively). A recent study reviewed the MNI coordinates of ATL activations for general semantic from 8 previous fMRI studies and found an average y MNI of -13.3 ± 4.9 (Rice et al., 2018), that is far more anterior than the presently highlighted AntFG face region. This last fMRI study also found bilateral ATL cluster responding to cross-modal person knowledge far anterior to our AntFG face region (y MNI coordinates between 3 and 7).

Given the above mentioned characteristics of the right AntFG face region (anatomical proximity with classical ATL semantic regions, strong functional connectivity with the MTL) and the in-depth investigation reported here, we therefore propose that this region, along with its role in unfamiliar face discrimination, is a critical hub located at the interface between posterior face-selective (modality-specific) VOTC regions, MTL regions involved in episodic memory encoding and ATL regions involved in cross-modal person-recognition and semantic memory associations.

Data availability statement

The data that support the findings of this study are available upon reasonable request from the corresponding author. The data are not publicly available due to privacy or ethical restrictions.

Declaration of Competing Interest

The authors declare no potential conflict of interest.

Credit authorship contribution statement

Angélique Volfart: Formal analysis, Data curation, Investigation, Visualization, Writing – original draft, Writing – review & editing. **Xiaoqian Yan:** Formal analysis, Visualization, Writing – original draft, Writing – review & editing. **Louis Maillard:** Resources. **Sophie Colnat-Coulbois:** Resources. **Gabriela Hossu:** Resources. **Bruno Rossion:** Funding acquisition, Methodology, Supervision, Writing – original draft, Writing – review & editing. **Jacques Jonas:** Investigation, Methodology, Supervision, Writing – original draft, Writing – review & editing.

Acknowledgments

We thank subject DN for his willingness and motivation to perform the study. We thank Dr Jean-Pierre Vignal for sharing his observations during intracerebral electrical stimulations with subject DN. We thank Caroline Michel for the stimuli and behavioral tasks on famous face recognition, and H el ene Brissart for neuropsychological assessment of subject DN.

This work was supported by the Lorraine Universit e d'Excellence program and the Excellence of Science (EOS) program (HUMVISCAT-30991544). AV was supported by the University of Lorraine (MESRI doctoral grant) and later by a postdoctoral grant from the University of Louvain.

Supplementary materials

Supplementary material associated with this article can be found, in the online version, at [doi:10.1016/j.neuroimage.2022.118932](https://doi.org/10.1016/j.neuroimage.2022.118932).

References

- Allison, T., Ginter, H., McCarthy, G., Nobre, A.C., Puce, A., Luby, M., Spencer, D.D., 1994. Face recognition in human extrastriate cortex. *J. Neurophysiol.* 71, 821–825.
- Aron, O., Jonas, J., Colnat-Coulbois, S., Maillard, L., 2021. Language mapping using stereo electroencephalography: a review and expert opinion. *Front. Hum. Neurosci.* 15, 619521.
- Avidan, G., Tanzer, M., Hadj-Bouziane, F., Liu, N., Ungerleider, L.G., Behrmann, M., 2014. Selective dissociation between core and extended regions of the face processing network in congenital prosopagnosia. *Cereb. Cortex N. Y.* 24, 1565–1578.
- Axelrod, V., Yovel, G., 2013. The challenge of localizing the anterior temporal face area: a possible solution. *Neuroimage* 81, 371–380.
- Barragan-Jason, G., Besson, G., Ceccaldi, M., Barbeau, E.J., 2013. Fast and famous: looking for the fastest speed at which a face can be recognized. *Front. Psychol.* 4, 100.
- Barsics, C., 2014. Person recognition is easier from faces than from voices. *Psychol. Belg.* 54, 244–254.
- Barton, J.J.S., 2008. Structure and function in acquired prosopagnosia: lessons from a series of 10 patients with brain damage. *J. Neuropsychol.* 2, 197–225.
- Behrmann, M., Avidan, G., Gao, F., Black, S., 2007. Structural imaging reveals anatomical alterations in inferotemporal cortex in congenital prosopagnosia. *Cereb. Cortex* 17, 2354–2363.
- Binney, R.J., Embleton, K.V., Jefferies, E., Parker, G.J.M., Lambon Ralph, M.A., 2010. The ventral and inferolateral aspects of the anterior temporal lobe are crucial in semantic memory: evidence from a novel direct comparison of distortion-corrected fMRI, rTMS, and semantic dementia. *Cereb. Cortex* 20, 2728–2738.
- Blank, H., Wieland, N., von Kriegstein, K., 2014. Person recognition and the brain: merging evidence from patients and healthy individuals. *Neurosci. Biobehav. Rev.* 47, 717–734.
- Bodamer, J., 1947. Die Prosop-Agnosie; die Agnosie des Physiognomieerkennens. *Arch. Psychiatr. Nervenkrankh. Ver. Mit. Z. Gesamte Neurol. Psychiatr.* 118, 6–53.
- Borchers, S., Himmelbach, M., Logothetis, N., Karnath, H.O., 2012. Direct electrical stimulation of human cortex — the gold standard for mapping brain functions? *Nat. Rev. Neurosci.* 13, 63–70.
- Bouvier, S.E., Engel, S.A., 2006. Behavioral deficits and cortical damage loci in cerebral achromatopsia. *Cereb. Cortex* 16, 183–191.
- Bruce, V., Young, A., 1986. Understanding face recognition. *Br. J. Psychol.* 77, 305–327.
- Busigny, T., Robaye, L., Dricot, L., Rossion, B., 2009. Right anterior temporal lobe atrophy and person-based semantic defect: a detailed case study. *Neurocase* 15, 485–508.
- Busigny, T., Rossion, B., 2010. Acquired prosopagnosia abolishes the face inversion effect. *Cortex* 46, 965–981.
- Busigny, T., Van Belle, G., Jemel, B., Hosein, A., Joubert, S., Rossion, B., 2014. Face-specific impairment in holistic perception following focal lesion of the right anterior temporal lobe. *Neuropsychologia* 56, 312–333.
- Caharel, S., Ramon, M., Rossion, B., 2014. Face familiarity decisions take 200 ms in the human brain: electrophysiological evidence from a Go/No-go speeded task. *J. Cogn. Neurosci.* 26, 81–95.
- Cardinale, F., Cossu, M., Castana, L., Casaceli, G., Schiariti, M.P., Miserochi, A., Fuschillo, D., Moscatto, A., Caborni, C., Arnulfo, G., 2012. Stereoelectroencephalography: surgical methodology, safety, and stereotactic application accuracy in 500 procedures. *Neurosurgery* 72, 353–366.
- Caspers, J., Zilles, K., Eickhoff, S.B., Schleicher, A., Mohlberg, H., Amunts, K., 2013. Cytoarchitectonical analysis and probabilistic mapping of two extrastriate areas of the human posterior fusiform gyrus. *Brain Struct. Funct.* 218, 511–526.
- Catenoix, H., Magnin, M., Manguiere, F., Ryvlin, P., 2011. Evoked potential study of hippocampal efferent projections in the human brain. *Clin. Neurophysiol.* 122, 2488–2497.
- Chau, A.M.T., Stewart, F., Gragnaniello, C., 2014. Sulcal and gyral anatomy of the basal occipital-temporal lobe. *Surg. Radiol. Anat.* 36, 959–965.
- Chen, Y., Chen, K., Ding, J., Zhang, Y., Yang, Q., Lv, Y., Guo, Q., Han, Z., 2019. Neural substrates of amodal and modality-specific semantic processing within the temporal lobe: a lesion-behavior mapping study of semantic dementia. *Cortex* 120, 78–91.
- Cohen, A.L., Soussand, L., Corrow, S.L., Martinaud, O., Barton, J.J.S., Fox, M.D., 2019. Looking beyond the face area: lesion network mapping of prosopagnosia. *Brain* 142, 3975–3990.
- Collins, J.A., Koski, J.E., Olson, I.R., 2016. More than meets the eye: the merging of perceptual and conceptual knowledge in the anterior temporal face area. *Front. Hum. Neurosci.* 10, 189.
- Collins, J.A., Olson, I.R., 2014. Beyond the FFA: the role of the ventral anterior temporal lobes in face processing. *Neuropsychologia* 61, 65–79.
- Cosseddu, M., Gazzina, S., Borroni, B., Padovani, A., Gainotti, G., 2018. Multimodal face and voice recognition disorders in a case with unilateral right anterior temporal lobe atrophy. *Neuropsychology* 32, 920–930.
- Crawford, J.R., Garthwaite, P.H., 2002. Investigation of the single case in neuropsychology: confidence limits on the abnormality of test scores and test score differences. *Neuropsychologia* 40, 1196–1208.
- Crawford, J.R., Howell, D.C., 1998. Comparing an individual's test score against norms derived from small samples. *Clin. Neuropsychol.* 12, 482–486.
- Davidoff, J., Landis, T., 1990. Recognition of unfamiliar faces in prosopagnosia. *Neuropsychologia* 28, 1143–1161.
- Davies-Thompson, J., Pancaroglu, R., Barton, J., 2014. Acquired prosopagnosia: structural basis and processing impairments. *Front. Biosci.* 6, 159–174.
- De Renzi, E., Faglioni, P., Grossi, D., Nichelli, P., 1991. Apperceptive and associative forms of prosopagnosia. *Cortex* 27, 213–221.
- Delvenne, J.F., Seron, X., Coyette, F., Rossion, B., 2004. Evidence for perceptual deficits in associative visual (prosop)agnosia: a single-case study. *Neuropsychologia* 42, 597–612.
- Desmurget, M., Song, Z., Mottolese, C., Sirigu, A., 2013. Re-establishing the merits of electrical brain stimulation. *Trends Cogn. Sci.* 17, 442–449.
- Dickerson, B.C., Eichenbaum, H., 2010. The episodic memory system: neurocircuitry and disorders. *Neuropsychopharmacology* 35, 86–104.
- Embleton, K.V., Haroon, H.A., Morris, D.M., Ralph, M.A.L., Parker, G.J.M., 2010. Distortion correction for diffusion-weighted MRI tractography and fMRI in the temporal lobes. *Hum. Brain Mapp.* 31, 1570–1587.
- Engell, A.D., McCarthy, G., 2011. The relationship of γ oscillations and face-specific ERPs recorded subdurally from occipitotemporal cortex. *Cereb. Cortex* 21, 1213–1221.
- Farah, M.J., 1990. *Visual Agnosia: Disorders of Object Recognition and What they tell us About Normal Vision*. MIT Press, Cambridge, Massachusetts.
- Finzi, D., Gomez, J., Nordt, M., Rezaei, A.A., Poltoratski, S., Grill-Spector, K., 2021. Differential spatial computations in ventral and lateral face-selective regions are scaffolded by structural connections. *Nat. Commun.* 12, 2278.
- Friedman, L., Glover, G.H. The FBIRN Consortium, 2006. Reducing interscanner variability of activation in a multicenter fMRI study: controlling for signal-to-fluctuation-noise-ratio (SFNR) differences. *Neuroimage* 33, 471–481.
- Gainotti, G., 2007. Different patterns of famous people recognition disorders in patients with right and left anterior temporal lesions: a systematic review. *Neuropsychologia* 45, 1591–1607.
- Gainotti, G., 2013a. Is the right anterior temporal variant of prosopagnosia a form of “associative prosopagnosia” or a form of “multimodal person recognition disorder”? *Neuropsychol. Rev.* 23, 99–110.
- Gainotti, G., 2013b. Laterality effects in normal subjects' recognition of familiar faces, voices and names. Perceptual and representational components. *Neuropsychologia* 51, 1151–1160.
- Gainotti, G., 2015. Is the difference between right and left ATls due to the distinction between general and social cognition or between verbal and non-verbal representations? *Neurosci. Biobehav. Rev.* 51, 296–312.
- Gainotti, G., Barbier, A., Marra, C., 2003. Slowly progressive defect in recognition of familiar people in a patient with right anterior temporal atrophy. *Brain* 126, 792–803.

- Gainotti, G., Ferraccioli, M., Marra, C., 2010. The relation between person identity nodes, familiarity judgment and biographical information. Evidence from two patients with right and left anterior temporal atrophy. *Brain Res.* 1307, 103–114.
- Gainotti, G., Marra, C., 2011. Differential contribution of right and left temporo-occipital and anterior temporal lesions to face recognition disorders. *Front. Hum. Neurosci.* 5, 55.
- Gao, X., Gentile, F., Rossion, B., 2018. Fast periodic stimulation (FPS): a highly effective approach in fMRI brain mapping. *Brain Struct. Funct.*
- Gauthier, I., Behrmann, M., Tarr, M.J., 1999. Can face recognition really be dissociated from object recognition? *J. Cogn. Neurosci.* 11, 349–370.
- Gauthier, I., Tarr, M.J., Moylan, J., Skudlarski, P., Gore, J.C., Anderson, A.W., 2000. The fusiform “face area” is part of a network that processes faces at the individual level. *J. Cogn. Neurosci.* 12, 495–504.
- Grande, K.M., Ihnen, S.K.Z., Arya, R., 2020. Electrical stimulation mapping of brain function: a comparison of subdural electrodes and stereo-EEG. *Front. Hum. Neurosci.* 14, 611291.
- Grill-Spector, K., Weiner, K.S., Kay, K., Gomez, J., 2017. The functional neuroanatomy of human face perception. *Annu. Rev. Vis. Sci.* 3, 167–196.
- Gschwind, M., Pourtois, G., Schwartz, S., Van De Ville, D., Vuilleumier, P., 2012. White-matter connectivity between face-responsive regions in the human brain. *Cereb. Cortex* 22, 1564–1576.
- Hagen, S., Jacques, C., Maillard, L.G., Colnat-Coulbois, S., Rossion, B., Jonas, J., 2020. Spatially dissociated intracerebral maps for face- and house-selective activity in the human ventral occipito-temporal cortex. *Cereb. Cortex* 30, 4026–4043.
- Hailstone, J.C., Ridgway, G.R., Bartlett, J.W., Goll, J.C., Buckley, A.H., Crutch, S.J., Warren, J.D., 2011. Voice processing in dementia: a neuropsychological and neuroanatomical analysis. *Brain* 134, 2535–2547.
- Hoffman, P.L., Ralph, M.A., 2018. From percept to concept in the ventral temporal lobes: graded hemispheric specialisation based on stimulus and task. *Cortex* 101, 107–118.
- Insnard, J., Taussig, D., Bartolomei, F., Bourdillon, P., Catenois, H., Chassoux, F., Chipaux, M., Clémenceau, S., Colnat-Coulbois, S., Denuelle, M., Derrey, S., Devaux, B., Dorfmueller, G., Gilard, V., Guenet, M., Job-Chapron, A.S., Landré, E., Lebas, A., Maillard, L., McGonigal, A., Minotti, L., Montavont, A., Navarro, V., Nica, A., Reyns, N., Scholly, J., Sol, J.C., Szurhaj, W., Trebuchon, A., Tyvaert, L., Valenti-Hirsch, M.P., Valton, L., Vignal, J.P., Sauleau, P., 2018. French guidelines on stereoelectroencephalography (SEEG). *Neurophysiol. Clin.* 48, 5–13.
- Jacques, C., Rossion, B., Volfart, A., Brissart, H., Colnat-Coulbois, S., Maillard, L.G., Jonas, J., 2020. The neural basis of rapid unfamiliar face individuation with human intracerebral recordings. *Neuroimage* 221, 117174.
- Jenison, A., Squire, L.R., 2012. Working memory, long-term memory, and medial temporal lobe function. *Learn. Mem.* 19, 15–25.
- Jenkins, R., Dowsett, A.J., Burton, A.M., 2018. How many faces do people know? *Proc. R. Soc. B* 285, 20181319.
- Jonas, J., Brissart, H., Hossu, G., Colnat-Coulbois, S., Vignal, J.P., Rossion, B., Maillard, L., 2018. A face identity hallucination (palinopsia) generated by intracerebral stimulation of the face-selective right lateral fusiform cortex. *Cortex* 99, 296–310.
- Jonas, J., Descoins, M., Koessler, L., Colnat-Coulbois, S., Sauvée, M., Guye, M., Vignal, J.P., Vespignani, H., Rossion, B., Maillard, L., 2012. Focal electrical intracerebral stimulation of a face-sensitive area causes transient prosopagnosia. *Neuroscience* 222, 281–288.
- Jonas, J., Jacques, C., Liu-Shuang, J., Brissart, H., Colnat-Coulbois, S., Maillard, L., Rossion, B., 2016. A face-selective ventral occipito-temporal map of the human brain with intracerebral potentials. *Proc. Natl. Acad. Sci. U. S. A.* 113, 4088–4097.
- Jonas, J., Rossion, B., 2021. Intracerebral electrical stimulation to understand the neural basis of human face identity recognition. *Eur. J. Neurosci.* n/a.
- Jonas, J., Rossion, B., Brissart, H., Frismand, S., Jacques, C., Hossu, G., Colnat-Coulbois, S., Vespignani, H., Vignal, J.P., Maillard, L., 2015. Beyond the core face-processing network: intracerebral stimulation of a face-selective area in the right anterior fusiform gyrus elicits transient prosopagnosia. *Cortex* 72, 140–155.
- Joubert, S., Felician, O., Barbeau, E., Ranjeva, J.P., Christophe, M., Didic, M., Poncet, M., Ceccaldi, M., 2006. The right temporal lobe variant of frontotemporal dementia. *J. Neurol.* 253, 1447–1458.
- Kahn, I., Andrews-Hanna, J.R., Vincent, J.L., Snyder, A.Z., Buckner, R.L., 2008. Distinct cortical anatomy linked to subregions of the medial temporal lobe revealed by intrinsic functional connectivity. *J. Neurophysiol.* 100, 129–139.
- Kanwisher, N., McDermott, J., Chun, M.M., 1997. The fusiform face area: a module in human extrastriate cortex specialized for face perception. *J. Neurosci.* 17, 4302–4311.
- Kovács, G., 2020. Getting to know someone: familiarity, person recognition, and identification in the human brain. *J. Cogn. Neurosci.* 32, 2205–2225.
- Krix, A.C., Sauerland, M., Schreuder, M.J., 2017. Masking the identities of celebrities and personally familiar individuals: effects on visual and auditory recognition performance. *Perception* 46, 1133–1150.
- Krüger, G., Glover, G.H., 2001. Physiological noise in oxygenation-sensitive magnetic resonance imaging. *Magn. Reson. Med.* 46, 631–637.
- Lavan, N., Burston, L.F.K., Garrido, L., 2019. How many voices did you hear? Natural variability disrupts identity perception from unfamiliar voices. *Br. J. Psychol.* 110, 576–593.
- Lavan, N., Scott, S.K., McGettigan, C., 2016. Impaired generalization of speaker identity in the perception of familiar and unfamiliar voices. *J. Exp. Psychol. Gen.* 145, 1604–1614.
- Levine, D.N., Calvanio, R., 1989. Prosopagnosia: a defect in visual configural processing. *Brain Cogn.* 10, 149–170.
- Libby, L.A., Ekstrom, A.D., Ragland, J.D., Ranganath, C., 2012. Differential connectivity of perirhinal and parahippocampal cortices within human hippocampal subregions revealed by high-resolution functional imaging. *J. Neurosci.* 32, 6550–6560.
- Liu-Shuang, J., Norcia, A.M., Rossion, B., 2014. An objective index of individual face discrimination in the right occipito-temporal cortex by means of fast periodic oddball stimulation. *Neuropsychologia* 52, 57–72.
- Lochy, A., Jacques, C., Maillard, L., Colnat-Coulbois, S., Rossion, B., Jonas, J., 2018. Selective visual representation of letters and words in the left ventral occipito-temporal cortex with intracerebral recordings. *Proc. Natl. Acad. Sci.* 115, 7595–7604.
- Lorenz, S., Weiner, K.S., Caspers, J., Mohlberg, H., Schleicher, A., Bludau, S., Eickhoff, S.B., Grill-Spector, K., Zilles, K., Amunts, K., 2017. Two new cytoarchitectonic areas on the human mid-fusiform gyrus. *Cereb. Cortex* 27, 373–385.
- Maher, S., Ekstrom, T., Ongur, D., Levy, D.L., Norton, D.J., Nickerson, L.D., Chen, Y., 2019. Functional disconnection between the visual cortex and right fusiform face area in schizophrenia. *Schizophr. Res.*
- Meadows, J.C., 1974. The anatomical basis of prosopagnosia. *J. Neurol. Neurosurg. Psychiatry* 37, 489–501.
- Mion, M., Patterson, K., Acosta-Cabrero, J., Pengas, G., Izquierdo-Garcia, D., Hong, Y.T., Fryer, T.D., Williams, G.B., Hodges, J.R., Nestor, P.J., 2010. What the left and right anterior fusiform gyri tell us about semantic memory. *Brain* 133, 3256–3268.
- Murphy, K., Bodurka, J., Bandettini, P.A., 2007. How long to scan? The relationship between fMRI temporal signal to noise ratio and necessary scan duration. *Neuroimage* 34, 565–574.
- Nasr, S., Tootell, R.B.H., 2012. Role of fusiform and anterior temporal cortical areas in facial recognition. *Neuroimage* 63, 1743–1753.
- Norcia, A.M., Appelbaum, L.G., Ales, J.M., Cottareau, B.R., Rossion, B., 2015. The steady-state visual evoked potential in vision research: a review. *J. Vis.* 15, 4.
- Omar, R., Rohrer, J.D., Hailstone, J.C., Warren, J.D., 2011. Structural neuroanatomy of face processing in frontotemporal lobar degeneration. *J. Neurol. Neurosurg. Psychiatry* 82, 1341–1343.
- Onitsuka, T., Shenton, M.E., Kasai, K., Nestor, P.G., Toner, S.K., Kikinis, R., Jolesz, F.A., McCarley, R.W., 2003. Fusiform gyrus volume reduction and facial recognition in chronic schizophrenia. *Arch. Gen. Psychiatry* 60, 349–355.
- Parvizi, J., Jacques, C., Foster, B.L., Withoft, N., Rangarajan, V., Weiner, K.S., Grill-Spector, K., 2012. Electrical stimulation of human fusiform face-selective regions distorts face perception. *J. Neurosci.* 32, 14915–14920.
- Penfield, W., 1958. The excitable cortex in conscious man. In: Thomas, C.C. (Ed.), *The Sherrington Lectures*. Liverpool University Press, Springfield, Ill.
- Penfield, W., 1975. The mind and the brain. In: Worden, F.G., Swazey, J.P., Adelman, G. (Eds.), *The Neurosciences, Paths of Discovery*. MIT Press, pp. 437–454.
- Persichetti, A.S., Denning, J.M., Gots, S.J., Martin, A., 2021. A data-driven functional mapping of the anterior temporal lobes. *J. Neurosci.*
- Puce, A., Allison, T., McCarthy, G., 1999. Electrophysiological studies of human face perception. III: effects of top-down processing on face-specific potentials. *Cereb. Cortex* 9, 445–458.
- Pyles, J.A., Verstynen, T.D., Schneider, W., Tarr, M.J., 2013. Explicating the face perception network with white matter connectivity. *PLoS One* 8, 61611.
- Rajimehr, R., Young, J.C., Tootell, R.B.H., 2009. An anterior temporal face patch in human cortex, predicted by macaque maps. *Proc. Natl. Acad. Sci. U. S. A.* 106, 1995–2000.
- Rangarajan, V., Hermes, D., Foster, B.L., Weiner, K.S., Jacques, C., Grill-Spector, K., Parvizi, J., 2014. Electrical stimulation of the left and right human fusiform gyrus causes different effects in conscious face perception. *J. Neurosci.* 34, 12828–12836.
- Retter, T.L., Rossion, B., 2016. Uncovering the neural magnitude and spatio-temporal dynamics of natural image categorization in a fast visual stream. *Neuropsychologia* 91, 9–28.
- Retter, T.L., Rossion, B., Schiltz, C., 2021. Harmonic amplitude summation for frequency-tagging analysis. *J. Cogn. Neurosci.* 1–22.
- Rice, G.E., Hoffman, P., Binney, R.J., Lambon Ralph, M.A., 2018. Concrete versus abstract forms of social concept: an fMRI comparison of knowledge about people versus social terms. *Philos. Trans. R. Soc. B Biol. Sci.* 373, 20170136.
- Rice, G.E., Lambon Ralph, M.A., Hoffman, P., 2015. The roles of left versus right anterior temporal lobes in conceptual knowledge: an ALE meta-analysis of 97 functional neuroimaging studies. *Cereb. Cortex* 25, 4374–4391.
- Ritaccio, A.L., Brunner, P., Schalk, G., 2018. Electrical stimulation mapping of the brain: basic principles and emerging alternatives. *J. Clin. Neurophysiol. Off. Publ. Am. Electroencephalogr. Soc.* 35, 86–97.
- Rossion, B., 2014. Understanding face perception by means of prosopagnosia and neuroimaging. *Front. Biosci. Elite Ed.* 6, 258–307.
- Rossion, B., 2018. Damasio’s error – prosopagnosia with intact within-category object recognition. *J. Neuropsychol.*
- Rossion, B., Caldara, R., Seghier, M., Schuller, A.M., Lazeyras, F., Mayer, E., 2003. A network of occipito-temporal face-sensitive areas besides the right middle fusiform gyrus is necessary for normal face processing. *Brain* 126, 2381–2395.
- Rossion, B., Hanseeuw, B., Dricot, L., 2012. Defining face perception areas in the human brain: a large-scale factorial fMRI face localizer analysis. *Brain Cogn.* 79, 138–157.
- Rossion, B., Jacques, C., Jonas, J., 2018. Mapping face categorization in the human ventral occipitotemporal cortex with direct neural intracranial recordings. *Ann. N. Y. Acad. Sci.*
- Rossion, B., Michel, C., 2018. Normative accuracy and response time data for the computerized Benton Facial Recognition Test (BFRT-c). *Behav. Res. Methods* 50, 2442–2460.
- Rossion, B., Retter, T.L., Liu-Shuang, J., 2020. Understanding human individuation of unfamiliar faces with oddball fast periodic visual stimulation and electroencephalography. *Eur. J. Neurosci.* 52, 4283–4344.
- Rossion, B., Schiltz, C., Robaye, L., Pirenne, D., Crommelinck, M., 2001. How does the brain discriminate familiar and unfamiliar faces?: a PET study of face categorical perception. *J. Cogn. Neurosci.* 13, 1019–1034.
- Rossion, B., Torfs, K., Jacques, C., Liu-Shuang, J., 2015. Fast periodic presentation of natural images reveals a robust face-selective electrophysiological response in the human brain. *J. Vis.* 15, 1–18.

- Salado, A.L., Koessler, L., De Mijolla, G., Schmitt, E., Vignal, J.P., Civit, T., Tyvaert, L., Jonas, J., Maillard, L.G., Colnat-Coulbois, S., 2017. sEEG is a safe procedure for a comprehensive anatomic exploration of the insula: a retrospective study of 108 procedures representing 254 transopercular insular electrodes. *Oper. Neurosurg.* 14, 1–8.
- Schalk, G., Kapeller, C., Guger, C., Ogawa, H., Hiroshima, S., Lafer-Sousa, R., Saygin, Z.M., Kamada, K., Kanwisher, N., 2017. Facephenes and rainbows: causal evidence for functional and anatomical specificity of face and color processing in the human brain. *Proc. Natl. Acad. Sci.* 114, 12285–12290.
- Schrouff, J., Raccach, O., Baek, S., Rangarajan, V., Salehi, S., Mourão-Miranda, J., Helili, Z., Daitch, A.L., Parvizi, J., 2020. Fast temporal dynamics and causal relevance of face processing in the human temporal cortex. *Nat. Commun.* 11, 1–13.
- Sergent, J., Poncet, M., 1990. From covert to overt recognition of faces in a prosopagnosic patient. *Brain* 113, 989–1004.
- Sergent, J., Signoret, J.L., 1992. Functional and anatomical decomposition of face processing: evidence from prosopagnosia and PET study of normal subjects. *Philos. Trans. R. Soc. Lond. B Biol. Sci.* 335, 55–61.
- Snowden, J.S., Harris, J.M., Thompson, J.C., Kobylecki, C., Jones, M., Richardson, A.M., Neary, D., 2018. Semantic dementia and the left and right temporal lobes. *Cortex* 188–203.
- Snowden, J.S., Thompson, J.C., Neary, D., 2012. Famous people knowledge and the right and left temporal lobes. *Behav. Neurol.* 25, 35–44.
- So, E.L., Alwaki, A., 2018. A guide for cortical electrical stimulation mapping. *J. Clin. Neurophysiol.* 35, 98–105.
- Talairach, J., Bancaud, J., 1973. Stereotaxic approach to epilepsy: methodology of anatomic-functional stereotaxic investigations. *Prog. Neurol. Surg.* 5, 297–354.
- Trébuchon, A., Chauvel, P., 2016. Electrical stimulation for seizure induction and functional mapping in stereoelectroencephalography. *J. Clin. Neurophysiol.* 33, 511–521.
- van Doorn, J., van den Bergh, D., Böhm, U., Dablander, F., Derks, K., Draws, T., Etz, A., Evans, N.J., Gronau, Q.F., Haaf, J.M., Hinne, M., Kucharský, Š., Ly, A., Marsman, M., Matzke, D., Gupta, A.R.K.N., Sarafoglou, A., Stefan, A., Voelkel, J.G., Wagenmakers, E.J., 2021. The JASP guidelines for conducting and reporting a Bayesian analysis. *Psychon. Bull. Rev.* 28, 813–826.
- Visser, M., Embleton, K.V., Jefferies, E., Parker, G.J.M., Lambon Ralph, M.A., 2010. The inferior, anterior temporal lobes and semantic memory clarified: novel evidence from distortion-corrected fMRI. *Neuropsychologia* 48, 1689–1696.
- Visser, M., Jefferies, E., Embleton, K.V., Lambon Ralph, M.A., 2012. Both the middle temporal gyrus and the ventral anterior temporal area are crucial for multimodal semantic processing: distortion-corrected fMRI evidence for a double gradient of information convergence in the temporal lobes. *J. Cogn. Neurosci.* 24, 1766–1778.
- Visser, M.L., Ralph, M.A., 2011. Differential contributions of bilateral ventral anterior temporal lobe and left anterior superior temporal gyrus to semantic processes. *J. Cogn. Neurosci.* 23, 3121–3131.
- Wandell, B.A., 2011. The neurobiological basis of seeing words. *Ann. N. Y. Acad. Sci.* 1224, 63–80.
- Wang, Y., Metoki, A., Smith, D.V., Medaglia, J.D., Zang, Y., Benear, S., Popal, H., Lin, Y., Olson, I.R., 2020. Multimodal mapping of the face connectome. *Nat. Hum. Behav.* 4, 397–411.
- Weiner, K.S., Grill-Spector, K., 2012. The improbable simplicity of the fusiform face area. *Trends Cogn. Sci.* 16, 251–254.
- Weiner, K.S., Grill-Spector, K., 2015. The evolution of face processing networks. *Trends Cogn. Sci.* 19, 240–241.
- Weiner, K.S., Zilles, K., 2016. The anatomical and functional specialization of the fusiform gyrus. *Neuropsychologia* 83, 48–62.
- Wiser, A.K., Andreasen, N.C., O’Leary, D.S., Crespo-Facorro, B., Boles-Ponto, L.L., Watkins, G.L., Hichwa, R.D., 2000. Novel vs. well-learned memory for faces: a positron emission tomography study. *J. Cogn. Neurosci.* 12, 255–266.
- Yan, X., Zimmermann, F.G., Rossion, B., 2020. An implicit neural familiar face identity recognition response across widely variable natural views in the human brain. *Cogn. Neurosci.* 1–14.
- Young, A.W., Frühholz, S., Schweinberger, S.R., 2020. Face and voice perception: understanding commonalities and differences. *Trends Cogn. Sci.* 24, 398–410.
- Zhang, W., Wang, J., Fan, L., Zhang, Y., Fox, P.T., Eickhoff, S.B., Yu, C., Jiang, T., 2016. Functional organization of the fusiform gyrus revealed with connectivity profiles. *Hum. Brain Mapp.* 37, 3003–3016.
- Zimmermann, F.G.S., Yan, X., Rossion, B., 2019. An objective, sensitive and ecologically valid neural measure of rapid human individual face recognition. *R. Soc. Open Sci.* 6, 181904.